Land-use, hydrological and geochemical drivers of greenhouse gas dynamics in eleven subtropical streams

Luke F. Andrews

February 2020

Supervisor: Professor Isaac Santos

Co–Supervisor: PhD candidate Shane White

Southern Cross University

School of Environment, Science and Engineering

Disclaimer

I certify that the work presented in the thesis, to the best of my knowledge and belief, is original, except as acknowledged in the text, and that the material has not been submitted, either in whole or part, for a degree at this or any other university.

I acknowledge that I have read and understood the university's rules and requirements relating to the awarding of my honours degree and to my thesis. I certify that I have complied with these.

Candidate Name: Luke Andrews

Date: 24/01/2020

Cover photographs: View of contrasting land uses within a freshwater catchment in the Coffs Harbour region. Photo credit: Shane White (2019).

Acknowledgements

Firstly, I would like to give thanks to Professor Isaac Santos and Shane White for their invaluable expertise and guidance throughout the course of research. Their willingness to give time in providing feedback has been very much appreciated.

A special thanks is also given to Praktan Wadnerkar whose efforts and expertise were integral to the completion of this project. I would also like to acknowledge the valuable contributions from Xiaogang Chen, Rogger Correa, Ceylena Holloway and Rebecca Woodrow for their lab support and processing of samples in the field.

Abstract

Freshwater systems are recognised as a significant source of greenhouse gases (GHGs) to the atmosphere (CO_2, N_2O and CH_4). GHGs emissions from freshwater streams are poorly quantified in sub-tropical climates, especially in the southern hemisphere where land use is rapidly changing. Here, we examined the concentration, drivers, and potential flux of CO_2, N_2O and CH_4 from 11 Australian freshwater streams with varying catchment land-uses yet similar hydrology, geomorphology and climate. These sub-tropical streams were an atmospheric source of CO_2 (74 ± 39 mol m^{-2} d^{-1}), CH_4 (0.04 ± 0.06 mmol m^{-2} d^{-1}) and N_2O (4.01 ± 5.98 µmol m^{-2} d^{-1}). CO_2 accounted for ~97% of all CO_2-equivalent emissions with CH_4 (~1.5%) and N_2O (~1.5%) playing a minor role. The episodic wet climate in sub-tropical Australia drove changes in stream GHGs through the release of soil NO_X and DOC following rainfall events. Groundwater discharge as traced by radon was not a source of CO_2 and CH_4, but seemed to influence N_2O dynamics. CO_2 and CH_4 increased with catchment forest cover during the wet period, while N_2O and CH_4 increased with agricultural catchment area during the dry period. Overall, this study shows how DOC and NO_X, land-use, and rainfall events interact to drive spatial and temporal dynamics in stream greenhouse gases in sub-tropical streams. These findings have implications for improving current global outgassing estimations of GHGs from streams.

Keywords: Climate change, landscape modification, Carbon Dioxide, Methane and Nitrous oxide.

Contents

List of Figures

List of Tables

1. Introduction

In light of current climate change predictions, there has been increased importance placed on developing comprehensive and robust accounts of natural and anthropogenic greenhouse-gas (GHG) fluxes (Borges et al., 2015). Inland streams have been recognised as an important source of GHGs, especially CO_2 due to its role in global carbon cycling (Cole et al., 2007; Aufdenkampe et al., 2011; Marx et al., 2017; Drake et al., 2018). Current estimates show that of the 5.1 Pg y^{-1} of terrestrially derived carbon exported into continental waters, only 0.95 Pg y^{-1} reaches the ocean (Drake et al., 2018). This lost carbon is attributed to the outgassing of carbon dioxide (~97%) (CO_2) and methane (~3%) (CH_4) at a rate of 3.9 Pg y^{-1} (Drake et al., 2018; Marx et al., 2017; Sawakuchi et al., 2017). However, limited direct measurements of CO_2 and spatiotemporal coverage have been identified as major knowledge gaps in current outgassing estimations (Cole et al., 2007). In order to provide more robust carbon fluxes estimates further research is required.

N_2O is also considered an important contributor to GHG evasion from streams (Beaulieu et al., 2010). Denitrification mediated by microbes has been identified as the major source of N_2O in streams (Marzadri et al., 2017). Current flux estimates from global river systems vary from 0.68 Tg N-N_2O yr^{-1} (Beaulieu et al., 2010) to 1.05 N-N_2O yr^{-1} (Seitzinger et al., 2010). While these absolute emission estimates for N_2O are far lower than 3.9 Pg y^{-1} for stream CO_2 emissions (Drake et al., 2018), N_2O has up to 300 times the sustained warming potential (SWP) of CO_2, making it a far more potent GHG (Maavara et al., 2019). However, quantifying N_2O stream emissions through upscaling is difficult and debated due to a lack of high resolution data and inadequate collection of geochemical parameters that drive nitrification and denitrification processes (Quick et al., 2019).

At a local scale, GHG fluxes are temporally and spatially dynamic driven by geochemical factors that are often attributed to the upstream catchment landscape (Marx et al., 2017; Jeffrey et al., 2018). For instance, CO_2 and CH_4 dynamics have been shown to be associated with a catchment's net ecosystem production (NEP) which represents the total amount of organic matter available for storage or export after net ecosystem respiration (Atkins et al., 2017; Borges et al., 2018a; Borges et al., 2015). Organic matter is used in microbial metabolism generating aqueous CO_2 and CH_4 that enter streams via runoff through the soil

zone, groundwater discharge, or in-stream respiration (Bodmer et al., 2016; Marx et al., 2017; Maher et al., 2019). Similarly, N_2O generation and stream fluxes are correlated with nitrogen export from the upland catchment landscape (Burgos et al., 2015). Under sub-oxic conditions, forms of dissolved inorganic nitrogen (DIN) are transformed through microbial metabolism generating N_2O as either an autochthonous (in-stream) or allochthonous (groundwater or runoff) source to streams (Quick et al., 2019). The flux of these geochemical components is highly dependent on catchment characteristics such as land use, climate and hydrology (Atkins et al., 2017; Petrone, 2010).

Hydrology plays an important role in the exchange of GHGs between the land, streams and atmosphere (Atkins et al., 2017; Looman et al., 2016b; Petrone et al., 2011). The delivery of solutes (OM, DIN) and aqueous forms of GHGs from the catchment landscape into streams is largely facilitated through flushing rainfall events (Dinsmore et al., 2013; Marx et al., 2017; Petrone et al., 2011; White et al., 2018; Jeffrey et al., 2018). These flushing events also tend to alter stream pH, temperature, and DO, which simultaneously affect the microbial production of GHGs in the hyporheic zone as well as their solubility and flux at the air-water interface (Borges et al., 2018a; Webb et al., 2016; Borges et al., 2015). Furthermore, runoff events tend to increase surface water velocity causing in-stream ebullition and generating enhanced rates of GHG evasion (Raymond et al., 2012; Borges et al., 2015). Sub-surface recharge also increases following rainfall, delivering groundwater supersaturated in CO_2 (Sadat-Noori et al., 2015), CH_4 (Borges et al., 2018b) , and N_2O (Quick et al., 2019) to streams. In the absence of rainfall or runoff, streams tend to have longer water residence times which allow for internal aquatic processes (such as microbial respiration, atmospheric diffusion and photodegradation) and slow groundwater seepage to exert a stronger influence on the surface water GHG pool (Marx et al., 2017; Smith and Kaushal, 2015). Given the importance of hydrology as a driver of GHG exports to and from the aquatic conduit, it is imperative to consider this aspect when developing large scale estimates.

Currently, the accuracy of global GHG emissions from streams is undermined due to a paucity of data in relation to regional evasion from smaller streams in tropical and subtropical latitudes, particularly in the southern hemisphere (Drake et al., 2018). In warmer tropical and subtropical systems, river discharge is often dominated by episodic rain events rather than seasonal cycles in temperate climates, potentially altering GHG dynamics (Looman et al., 2016b). Furthermore, the largest fraction of CO_2 evasion from inland waters has been shown to occur at low latitudes, emphasizing the need to increase the spatial coverage of GHG

investigations (Sawakuchi et al., 2017). This lack of spatial coverage also extends to upland streams which are underrepresented given that they comprise up to 90% of terrestrial drainage patterns worldwide (Drake et al., 2018; MacDonald and Coe, 2007). These streams are also important as they exhibit high surface area-to-volume ratios, which maximise the interface for GHG exchange with the atmosphere and facilitate high levels of loading from the adjacent landscape through the hyporheic zone (Comer-Warner et al., 2019). The uncertainties in current estimates are further refined by Drake et al. (2018) who suggest more studies need to be done in relation to low-order streams draining from continental margins with consideration of anthropogenic perturbation.

The impact of anthropogenic landscape modification on nutrient cycles within the aquatic environment has been extensively explored (Seitzinger et al., 2010; Canfield et al., 2010; White et al., 2018). However, this same level of information is not available linking GHGs evasion to land-use activities (Petrone, 2010; Marx et al., 2017). Until recently, the lateral transport of carbon from the land into streams and ocean has been considered a natural loop unaffected by land-use modification (Drake et al., 2018). Since pre-industrial times, anthropogenic perturbation has increased carbon loading to inland waters by as much as 1 Pg C yr^{-1} due to deforestation and agricultural intensification (as much 0.8 Pg C yr^{-1}) (Drake et al., 2018). Such activities contribute to soil disturbance, which facilitates the hydrologic export of nitrogen and carbon sources into inland waters (Bass et al., 2011; Bass et al., 2014). Additionally, urbanisation can impact stream geochemical cycling due to reduced hydrologic retention from impervious materials which may enhance loading of DOC (Petrone, 2010), NOx (Petrone et al., 2008) and potentially contribute to GHG production (Maher et al., 2019). Quantifying GHG fluxes from catchments which have undergone land-use change is crucial to not only further our understanding of mechanisms driving the natural carbon cycle but also for closing the carbon budget which currently neglects the influence of anthropogenic perturbation (Drake et al., 2018). Previous work four estuaries in the subtropical Coffs Harbour region found urban and agricultural land use decreased DOC loading and CO_2 outgassing (Looman et al., 2019). The following study hopes to build on this information and investigate how GHG dynamics in freshwater sub-catchments change in response to land use and hydrological conditions at a broader spatial scale.

1.1 Aims and objectives

This study aims to quantify the fluxes of GHGs (CO_2, CH_4 and N_2O) from streams across a catchment land-use gradient and varying hydrological regimes. I hypothesize that: (1) the

predominately agricultural and mixed modified catchments will have reduced lateral carbon fluxes (DOC) and hence lower CH_4 and CO_2 evasion due to modified hydrology; (2) catchments dominated by agricultural land will accentuate evasion rates of N_2O due to higher levels of NO_x; (3) periods of high hydrological connectivity will best capture inferences between land use and GHG fluxes; and (4) geochemical drivers will play a dominant role in GHG partitioning and fluxes irrespective of the hydrological regime. To assess these hypotheses, we measured the three main greenhouse gases across 11 subtropical creeks with varying land use yet similar climate, geomorphology and hydrologic regimes. This study builds on existing literature by: (1) Quantifying GHG fluxes from subtropical streams in the southern hemisphere; (2) Investigating geochemical drivers of GHG production in streams; (3) Comparing GHG fluxes in relation to catchment land use gradients to assess the influence of anthropogenic perturbation; and (4) Assess the influence of episodic wet-dry hydrology on GHG fluxes (5) We use radon to assess if stream GHGs are driven by surface runoff or groundwater discharge.

2. Material and Methods

2.1 Study sites

Sampling was conducted in 11 freshwater streams situated within the Coffs Harbour region on the east coast of Australia (Figure, 1). These freshwater catchments were selected due to their comparable geomorphology, climate, and hydrological characteristics, but contrasting land use (Figure, 1). The study region is situated between 30°10' S and 30°30'S along a narrow 80 km strip of land between the Great Diving Range and Pacific Ocean. Central to this area is the city of Coffs Harbour which has a humid subtropical climate with a mean temperature of 23°C and average annual rainfall of 1688 mm (Australian Bureau of Meteorology, 2019a). Local precipitation drainage in the area is predominately mediated by small hydrologically responsive streams of low Strahler order due to the geographic confinements of the region. Vegetation in the upper and middle catchment areas is dominated by remnant wet-sclerophyll and mixed rainforest (Coffs Harbour City Council, 2012). Moving into the lower catchment areas, vegetation is mainly restricted to the riparian zones, composed of *Eucalyptus*, *Casuarina* and *Melaleuca* species (Looman et al., 2019). Soils are of basaltic origin, typically well drained and display podzolic horizon features (Milford, 1999).

Parts of the study region has undergone significant landscape modification since the 1920's with widespread clearing of forests for urban, agricultural and forestry purposes (Looman et al., 2019). Land was originally cleared for banana plantations on the hillslopes and grazing on the erosional valley fills (Conrad et al., 2017). Since the 1970's the banana industry has been superseded by other intensive horticultural practices such as blueberry cultivation which have been linked to increased nitrogen loading in local streams (White et al., 2018). Population is concentrated around Coffs, Ferntree and Boambee catchments with population densities of $\geq$ 18 persons per km^2 (Looman et al., 2019). These factors have led to the development of the current landscape which displays mosaic patterns of urban (residential, commercial, industrial), agricultural (grazing and horticulture including banana plantations, blueberry farms and hothouses) and forest (managed and natural) land uses (Fig. 1). Earlier nitrate observations in regional streams were linked to agricultural land use (White et al., 2018), while observations in four regional estuaries found greater DOC and CO_2 in natural estuaries (Looman et al., 2019). Here, we build on earlier work by investigating freshwater sub-catchments at a broader spatial scale rather than the estuarine mixing gradient.

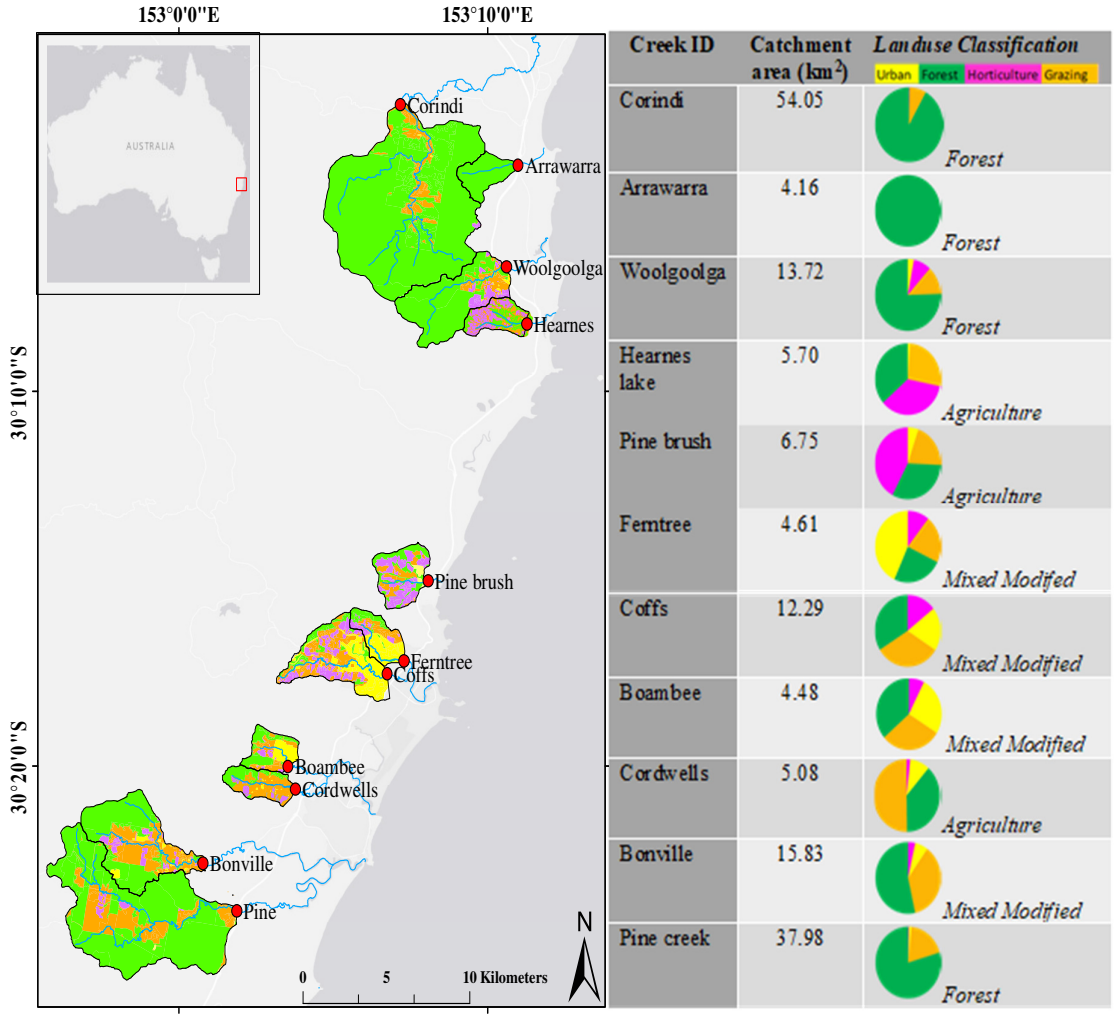

Figure 1. Map of study region with freshwater sub-catchment boundaries and sample sites indicated in red. Individual catchment land use classification on the right (north to south).

2.2 Sampling and analysis

Creek water samples were collected at weekly intervals from 10 January to 2 May 2019, totalling 15 samples per site. Sampling locations within streams were selected based on the upper limit of the tidal reach (salinity < 2.0 ppt) and hydro-geomorphology. During the first survey, four sites (Boambee, Cordwells, Bonville, and Woolgoolga) recorded salinity readings >2.0ppt, indicative of estuarine water penetration during extreme dry conditions. These outliers were removed from the dataset. Nutrients (DOC, nitrate + nitrite [NO_x]), GHGs (CO_2, CH_4, N_2O) and general water parameters (temperature (°C), salinity, pH, and dissolved

oxygen [DO]) were sampled from surface stream water on each sampling occasion using a peristaltic pump.

DOC samples were collected using polyethylene syringes, filtered through pre-combusted 0.7 µm GF/F filters (Whatman), and stored in 40 mL borosilicate vials (USP Type I) treated with 30 µL of H_3PO_4. Vials were stored at 3°C for laboratory analysis. Total organic carbon (TOC) concentrations were assessed using an Aurora 1030W TOC Analyser (Thermo Fisher Scientific, ConFLo IV). NO_x concentrations were determined colourimetrically on a Lachat Flow Injection Analyser (FIA). For that, water samples were collected in 10 mL polyethylene vials, filtered through a 0.7 µm glass fibre syringe filter and frozen for laboratory analysis. GHGs samples were collected by extracting 50 ml of water in five polyethylene syringes and introducing gas with known partial pressures to create a water-air headspace gradient for gas transfer. The headspace was then syringed into 1L tedlar gas (Supelco company) bags for analysis in a calibrated cavity ring down spectrometer (Picarro G2308) to determine CO_2, CH_4 and N_2O values in air. The partial pressures, concentrations, and percent saturation of the GHGs in water were calculated from gas-specific solubility constants as a function of salinity and temperature (Pierrot et al., 2009; Weiss and Price, 1980; Yamamoto et al., 1976). Groundwater contributions to the streams were assessed using the naturally occurring radioactive isotope radon (^{222}Rn; $Y_{1/2}$ = 3.83 days) (Burnett et al., 2001). Here, discrete samples were taken with 2 L HDPE plastic bottles which were sealed airtight until further analysis. Samples were run on a RAD7 (Durridge Company) in-air closed loop monitor, following methods outlined by Lee and Kim (2006).

2.3 Data interpretation and analysis

Upstream catchment boundaries and land-use characteristics (Fig 1) were identified using watershed delineation and data provided by the Coffs Harbour City Council Local Environment Plan (Parliamentary Counsel's Office, 2013) on ArcGIS Spatial Analyst (Version 10.5.1, ESRI). The classification of land-use was verified and adjusted using current satellite imagery from Google Earth (2019) and ground truthing. Several of the catchments had cleared pastured landscapes which was categorised as 'cleared/grazing agricultural land'. Catchments were then categorised into Forested, Agricultural (Cleared land + Horticulture) and Mixed Modified (Urban + Agriculture) according to % coverage of each land use within the freshwater catchments (> 75% forest = Forested, >50% horticulture or cleared land = Agricultural, <50% agriculture and <75% forest = Mixed Modified, Fig. 1). This method enabled a comparison of GHG observations to the degree and type of landscape modification.

Rainfall and wind speed data were obtained from the Coffs Harbour Airport station (059151). Runoff was determined from the Australian Landscape Water Balance model (AWRA-L) (BOM, 2019). Given only one rainfall station was available for hydrology comparisons, we assumed a homogenous parametrisation of daily runoff calculated from an average (mm m^{-2} day^{-1}) of all catchments. To determine stream surface area for discharge calculations, creek cross-section profiles were recorded at each creek. Changes in vertical stream profiles were recorded through weekly depth measurements taken centre-stream. Stream cross-section area was calculated using the trapezoidal rule ($A = \frac{x1+2x+x3}{4} \times width$) with velocity being determined from AWRA-L runoff data (BOM, 2019).

GHG water-atmosphere fluxes were determined using:

$$Flux\ (mmol\ m^{-2}d^{-1}) = k\ \alpha\ (C_w - C_{atm}) \qquad (1)$$

where k is the gas transfer velocity (m d^{-1}), α is the solubility constants for each respective GHG, C_w the concentration of the gas in water, and C_{atm} is the ambient partial atmospheric pressure. Ambient atmospheric pressures used for CO_2, N_2O, and CH_4 were 412 pm, 0.326 ppm, and 1.783 ppm, respectively, as observed from local air samples.

Gas transfer velocities were determined using two different empirical models to offer a range in possible emissions:

Raymond and Cole (2001): $k = 5.141u^{0.758}\ (Sc/660)^{-1/2}$ (2)

Borges et al. (2004): $k=1.91e^{0.35u}\ (Sc/600)^{-1/2}$ (3)

where k is the transfer velocity (cm h^{-1}), u is the wind speed at 10 meters above ground (m s^{-1}) obtained from BOM (2019), Sc is the Schmidt number of the gas at in situ temperature and salinity (Wanninkhof, 1992). Given that the sampling sites were typically surrounded by riparian vegetation, influence from wind speed was likely to be minimal, hence the above piston velocities were also calculated with respect to 0 km h^{-1} wind speeds. An average was derived of both models at 0 km h^{-1}.

Net exports (potential emissions to the atmosphere assuming oversaturated values degas to the atmosphere in the downstream estuaries) were calculated by multiplying discharge with the difference between observed stream concentrations and concentrations at equilibrium with the atmosphere. This approach allows for an estimate of the potential

emissions downstream of the observation site assuming the aquatic GHGs will approach atmospheric equilibrium following degassing downstream. CO_2 equivalent (CO_2-eq) emissions were also calculated using equations of solubility (Yamamoto et al., 1976), as well as 20 year sustained global warming potential (SGWP) estimations (Neubauer and Megonigal, 2015) with CO_2-eq (20yr) = $1CO_2 + 96CH_4 + 250N_2O$. Correlations between land-use, GHGs and physico-chemical drivers were analysed using IBM SPSS (25) Pearson's Correlation linear regressions (2-tailed, confidence interval: 0.05).

3. Results

3.1 Hydrological conditions, geochemical and ancillary parameters

Two contrasting hydrological regimes were observed across the 15-week sampling period: (1) a dry period with low rainfall (total of 86 mm in 63 days) and peak run off reaching 0.25 mm m^{-2} day^{-1}, and (2) a wet period (total of 327 mm in 41 days) with spikes in catchment runoff of up to 0.7 mm m^{-2} day^{-1} (Fig. 2). Rainfall for the whole sampling period (total of 413 mm) was below the historical average of 720 mm (BOM, 2019).

Streams during the dry period had higher temperatures, low DO (18 to 65 % saturation), lower pH and NO_x concentrations (0.4 to 10 µmol/L) (Table 1, Fig. 3). In comparison, during the wet period streams experienced higher DO (25.4 to 85.5 %), pH and NO_x (3 to 105 µmol/L) with temperatures decreasing moving into autumn (Figure 3). DOC concentrations exhibited no distinct trend throughout the sampling period ranging from 250 to 450 µmol/L (Fig. 3).

CO_2 ranged from 520 % at Hearnes Lake to 1637 % at Pine Creek (Fig. 4) peaking across most sites during the dry period before decreasing during the wet period (with the exception of the forested catchments) (Fig. 3). The general decrease in CO_2 moving into the wet period was substantiated by a significant inverse relationship with runoff ($p<0.01$, Fig. 5). Correlations with radon were only apparent during the dry period with CO_2 significantly increasing with ^{222}Rn (Fig. 6). Further, CO_2 exhibited a significant negative correlation with DO (Fig. 7, $p< 0.01$ appendix A, Table 1) and a significant positive linear relationship with DOC in both hydrological periods (Fig. 7, $p<0.05$, Table 2).

CH_4 was highly variable between sites ranging from 428 % at Hearnes Lake to 9448 % at Cordwells (Fig. 4). This variation was greatest during the dry period, with sites such as Cordwells (agricultural site) experiencing large spikes (>9389 %) at surveys 2, 5 and 7 (Fig.

3). Overall, moving into the wet period CH_4 decreased, exhibiting a significant inverse relationship with runoff (p=0.03, Fig. 5). In contrast to CO_2, CH_4 displayed no correlations to radon across either the dry or wet period (Figure 6). Further, as seen with CO2, CH4 also negatively correlated with DO throughout the dry and wet periods (Fig. 7. p<0.05, Table 2).

N_2O ranged from 115 % (Pine) to 190% (Boambee) during the dry period and from 119% (Corindi) to 1428 % (Woolgoolga) during the wet period (Fig. 3). The peak saturation observed at the Woolgoolga site was up to 10 times greater than other sites (Fig. 3). We suspect this is due to the site's location immediately downstream of a hot house facility and a limited flow path for N_2O to outgas. Transitioning into the wet period, N2O spiked at sample 11 across all catchments following consecutive days of >20 mm rain (Fig. 3). In contrast to CO_2 and CH_4, N_2O significantly increased with increasing runoff (p<0.01, Fig. 5) and in relation to ^{222}Rn (Fig. 6). Further, N_2O exhibited a significant positive correlation with NO_x concentrations across both hydrological regimes (Figure 7, p<0.01, Table 1) and with DOC during the wet period (Fig. 7, p=0.03, Table 1)

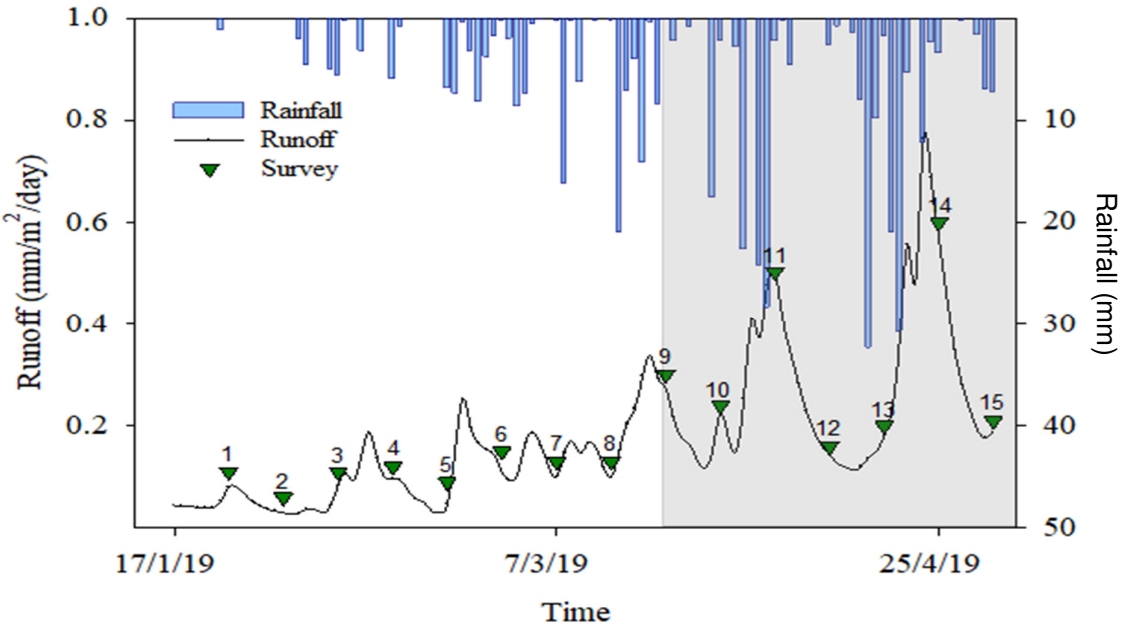

Figure 2. Time series of daily rainfall and average catchment runoff (AWRA-L data, BOM) over a 98-day sampling period in the Coffs Harbour region. Grey area denotes the wet period.

Table 1. Mean (± SD) physico-chemical parameters recorded from each freshwater sub-catchment with reference to corresponding land use classification.

Creek ID	Land Use Classification	Temp (°C)		pH		DO (%)		Conductivity (μScm^{-1})	
		Dry	Wet	Dry	Wet	Dry	Wet	Dry	Wet
Corindi	Forest	26.5±2.3	23.6±2.3	6.91±0.11	6.97±0.35	55.6±48.5	32.2±20.7	150±61	152±8
Arrawarra	Forest	25.5±3.2	23.5±2.3	6.96±0.21	7.26±0.46	43.2±20.7	52.8±12.7	265±92	247±28
Woolgoolga	Forest	27.2±1.9	23.4±2.2	6.98±0.12	7.09±0.38	41.4±18.8	69.2±26.5	268±61	293±39
Hearnes	Agriculture	25.4±1.8	22.6±2.1	7.02±0.22	7.37±0.49	44.8±14.9	78.3±14.9	329±220	391±131
Pinebrush	Agriculture	25.9±3.2	21.7±1.2	6.85±0.12	7.41±0.58	65.8±10.6	82.6±11.7	195±96	296±177
Ferntree	Mixed Modified	25.5±2.2	22.2±1.6	6.92±0.05	7.34±0.53	31.7±13.4	78.3±23.5	183±78	166±30
Coffs	Mixed Modified	25.3±2.1	22±0.9	6.8±0.12	7.24±0.49	24.3±10.5	70.4±17.4	217±209	180±40
Boambee	Mixed Modified	23.4±1.1	21.8±0.7	6.63±0.09	7.14±0.46	39.7±7.9	76.7±16.2	167±7	168±45
Cordwells	Agriculture	23.7±1.5	21.1±0.5	6.67±0.17	7.01±0.49	22.8±20.6	47.3±27.1	182±57	149±51
Bonville	Mixed Modified	23.3±1.2	20.7±0.8	6.61±0.09	7.11±0.42	62.2±2.6	85.5±2.4	88±19	70±3
Pine	Forest	24.0±1.4	20.31±1.0	6.33±0.17	6.68±0.33	18.4±7.4	29.1±10.1	97±77	167±237

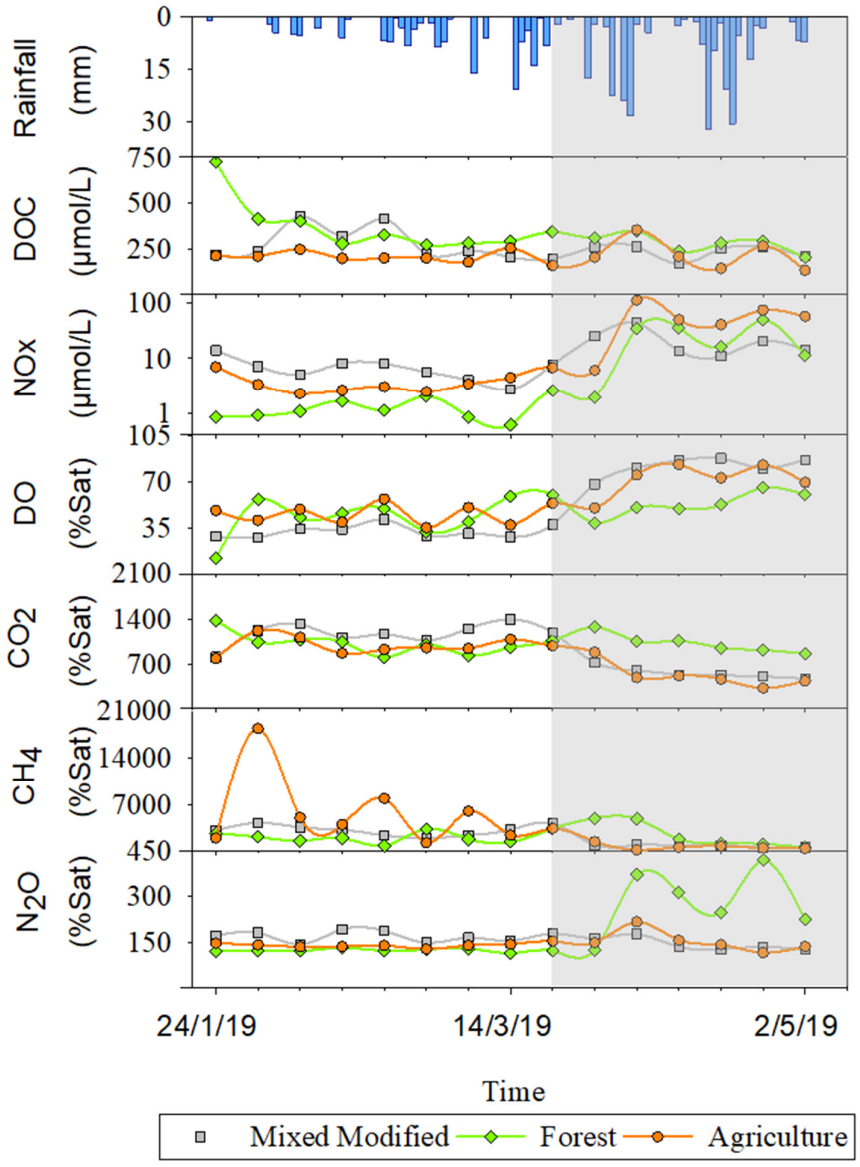

Figure 3. Time series of physico-chemical parameters and greenhouse gases recorded as means (n=4 mixed modified, n=3 agriculture, n=4 forest) according to catchment classification. Shaded area indicates wet hydrology period.

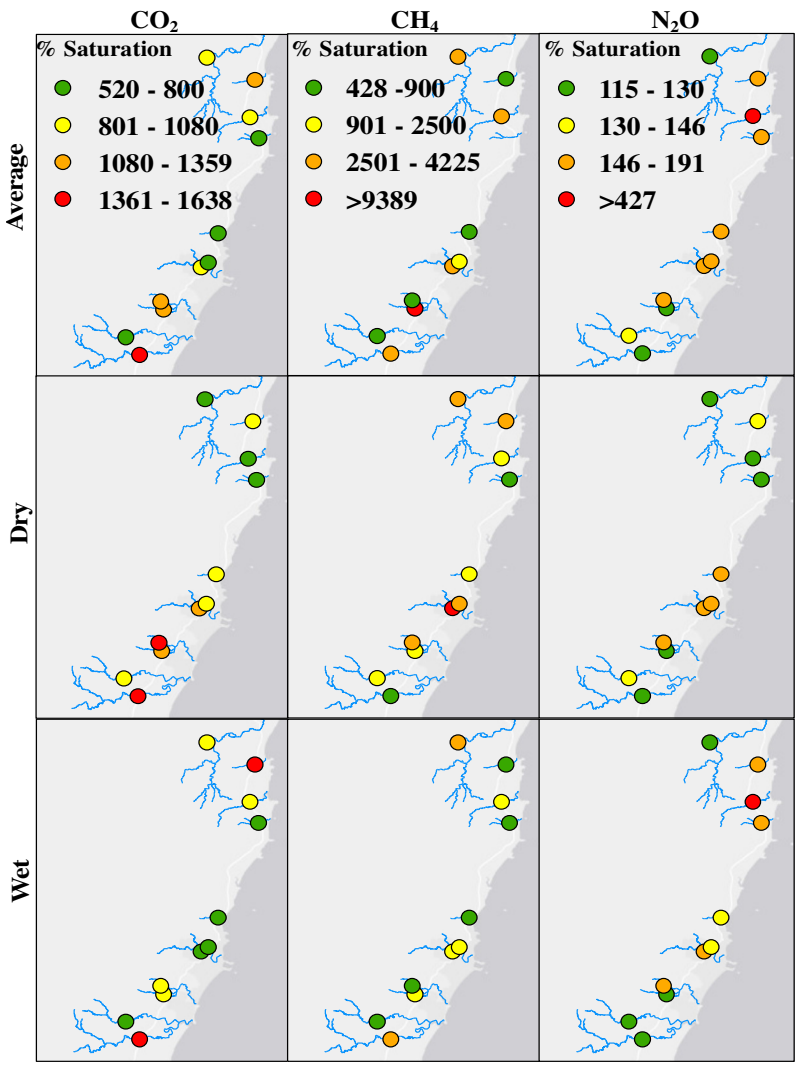

Figure 4. Mean greenhouse gas values (% saturation) for each sampling site according to hydrological period.

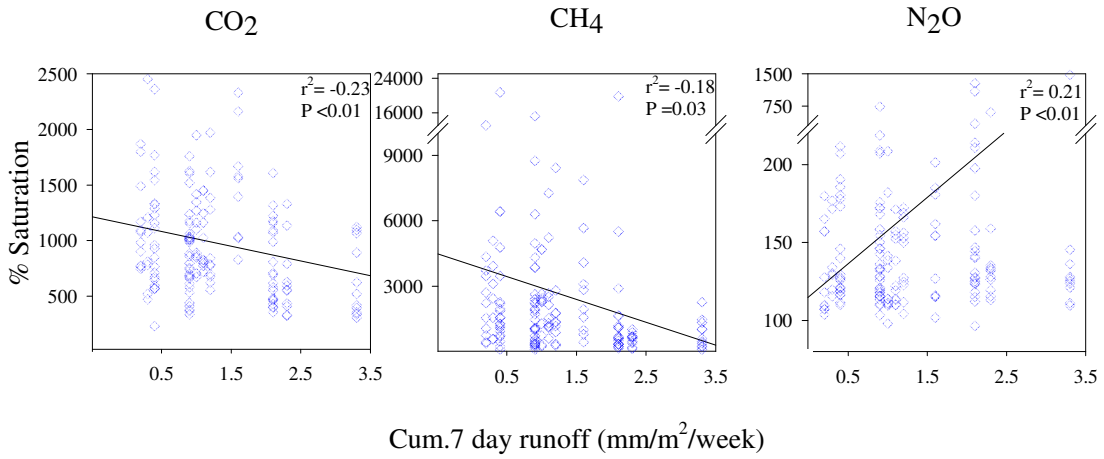

Figure 5. Scatter plot of mean GHG concentrations (% sat) versus 7-day cumulative runoff (mm/m^2/day) obtained from AWRA-L data, BOM. Lines indicate significance (Pearson's correlation 2-tailed, p = 0.05).

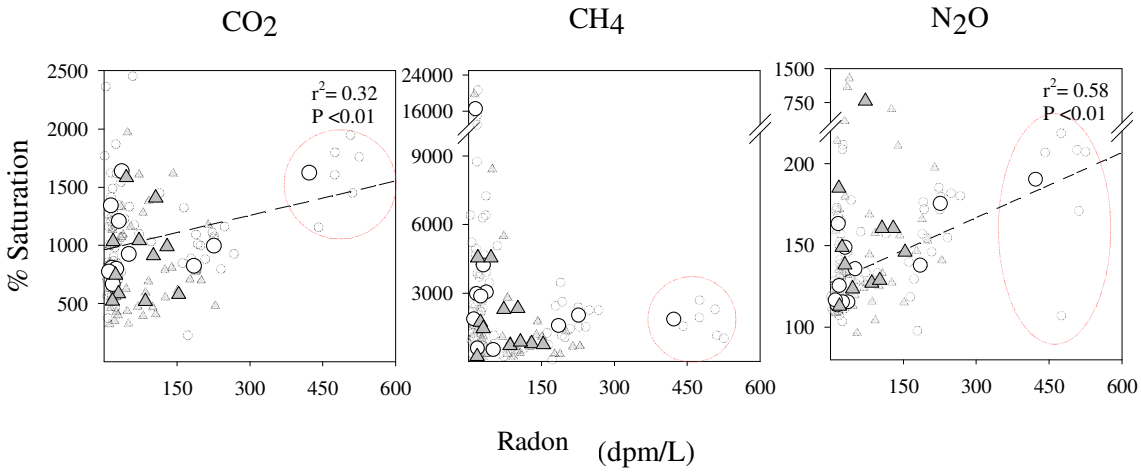

Figure 6. Scatter plot of mean (large symbols) GHG saturations (% sat) versus Radon (^{222}Rn). Smaller symbols show all data points. Dashed lines indicate significance including outliers (red circles) using Pearson's correlation (2-tailed, p = 0.05). Removing outliers results in CO_2 vs Rn ($p>0.05$, $r^2=0.22$) N_2O vs Rn ($p<0.05$ $r^2=0.49$).

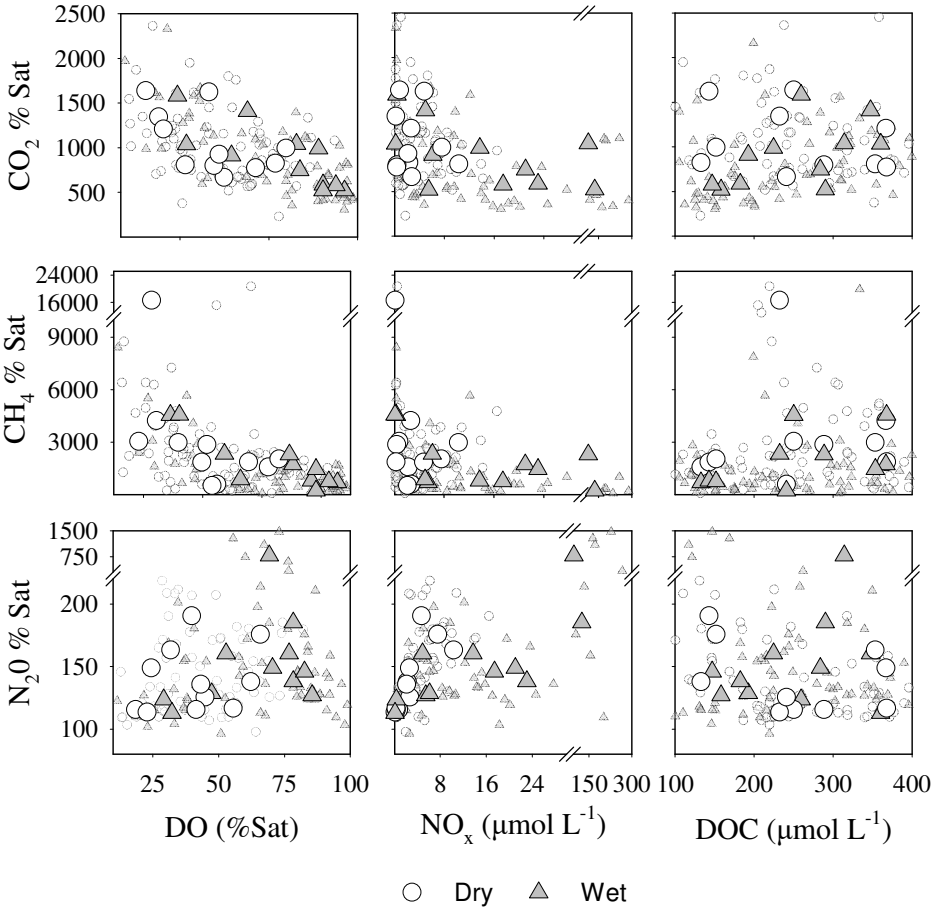

Figure 7. Scatter plot of mean (large symbols) GHG concentrations (% sat) versus ancillary measures (DO, NO_x and DOC). Smaller symbols show all data points, dry (n =84) and wet (n = 77). For all r^2 and *p* values see appendix A, Table 1.

3.2 Land use drivers of GHGS and fluxes

Land use and GHG correlations varied in relation to the governing hydrology period (Fig. 8). During the dry period no correlations were found between catchment land use and CO_2 (Fig. 8, Table 2). However, wet CO_2 values exhibited a significant positive correlation with forest area (% of catchment) ($p<0.01$, Table 2) and a negative correlation with increasing agriculture ($p<0.01$, Table 2) and mixed modified catchment area ($p<0.01$, Table 2). In contrast to CO_2, CH_4 increased significantly (Dry, $p=0.33$, Wet $p=0.047$, Table 2) with agricultural catchment area across both hydrological regimes (Fig. 8). A positive correlation was also evident during the wet period with increasing forested ($p=0.041$) and mixed modified ($p=0.041$) catchment area (Fig. 8). Whereas, N_2O showed a significant positive correlation with increasing agricultural and mixed modified catchment areas only during the dry period ($p=0.043$, Fig. 8).

Overall streams were a source of all three GHGs (Fig. 9). Fluxes mimicked the trends from the saturation percentages in relation to hydrology and land use (Fig. 9). On average, CO_2 fluxes in the present study were found to be 74 ± 39 mol m^{-2} d^{-1} and accounted for 97% of SWGP for all streams (Fig 9) CH_4 fluxes were highly variable with an average of 0.04 ± 0.06 mmol m^{-2} d^{-1} (Fig. 9). N_2O displayed a net-positive flux at an average rate of 4.01 ± 5.98 µmol m^{-2} d^{-1} (Fig. 9). It is also worth noting that CH_4 had a greater contribution to CO_2 eq emissions during the dry (1.94 % dry versus 1.11 % wet), while N_2O had a greater contribution during the wet (2.01 % wet versus 0.78 % dry) (Fig. 9).

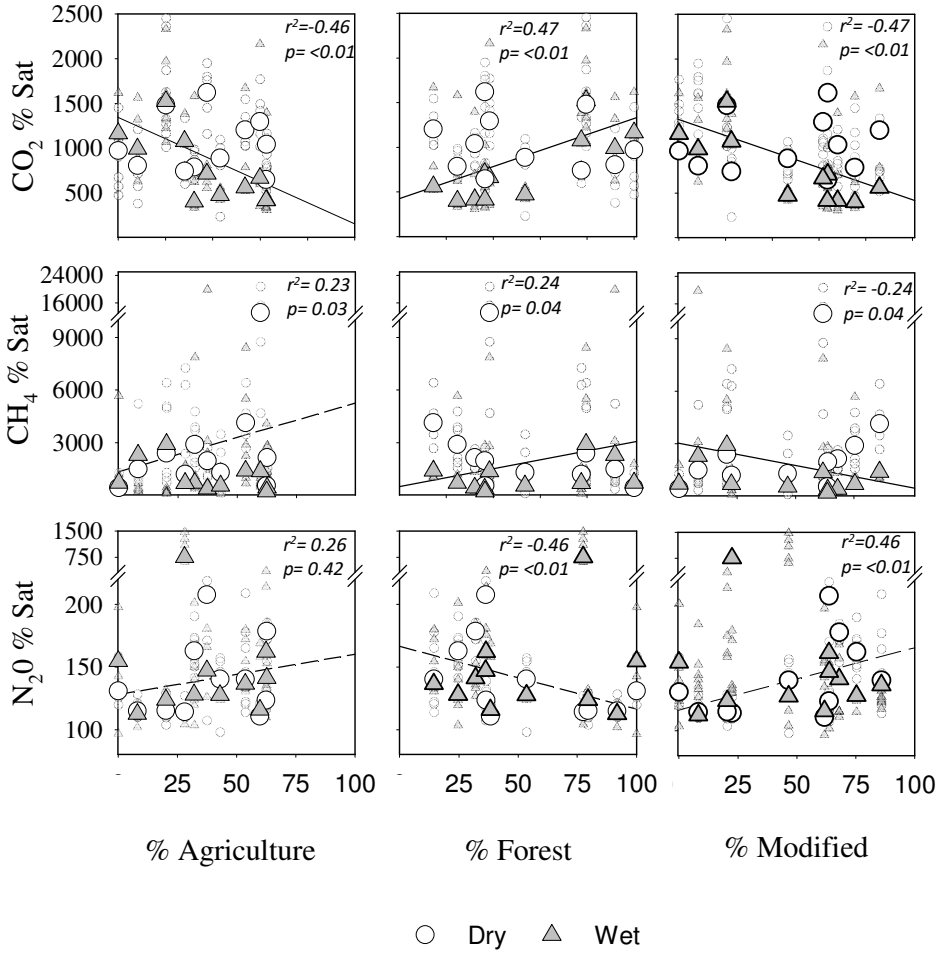

Figure 8. Scatter plot of median (large symbols) GHG concentrations (% sat) versus % land use according to catchment area. Smaller symbols show all data points. Dashed lines indicate significance (Pearson's correlation 2-tailed, $p < 0.05$) during the dry (n = 84) and solid lines during the wet (n = 77). For all r^2 and p values see appendix A, Table 1.

Table 2. Mean (± SD) air-atmosphere GHG fluxes in relation to two piston velocity models assuming 0 km/hr windspeed.

Piston velocity model		CO_2	CH_4	N_2O	CO_2	CH_4	N_2O
Borges (2004) $K=5.141u^{0.758}(Sc/660)^{-1/2}$	Agriculture	106.85 ±34.85	0.1 ±0.15	3.13 ±2.61	95.45 ±74.05	0.03 ±0.05	5.8 ±7.4
	Forest	53.91 ±28.83	0.02 ±0.03	0.67 ±0.32	101.13 ±42.43	0.05 ±0.09	14.46 ±33.61
	Mixed Modified	85.42 ±43.01	0.04 ±0.02	2.84 ±1.91	76.7 ±69.13	0.02 ±0.03	3.34 ±2.44
Raymond and Cole (2001) $K=1.91e^{0.35u}(Sc/660)^{-1/2}$	Agriculture	64.1 ±23.42	0.08 ±0.16	2.04 ±1.64	41.59 ±33.33	0.01 ±0.02	2.34 ±2.32
	Forest	67.93 ±36.22	0.03 ±0.03	1.09 ±0.67	84.79 ±32.54	0.04 ±0.06	8.59 ±17.05
	Mixed Modified	72.92 ±28.22	0.04 ±0.02	2.91 ±1.59	44.42 ±36.79	0.01 ±0.02	1.91 ±1.19
Average	Agriculture	85.48 ±26.3	0.09 ±0.15	2.59 ±2.05	68.52 ±53.34	0.02 ±0.04	4.07 ±4.79
	Forest	60.92 ±31.59	0.03 ±0.03	0.88 ±0.46	92.96 ±33.63	0.05 ±0.07	11.53 ±25.17
	Mixed Modified	79.17 ±34.74	0.04 ±0.02	2.88 ±1.67	60.56 ±52.42	0.02 ±0.02	2.62 ±1.76

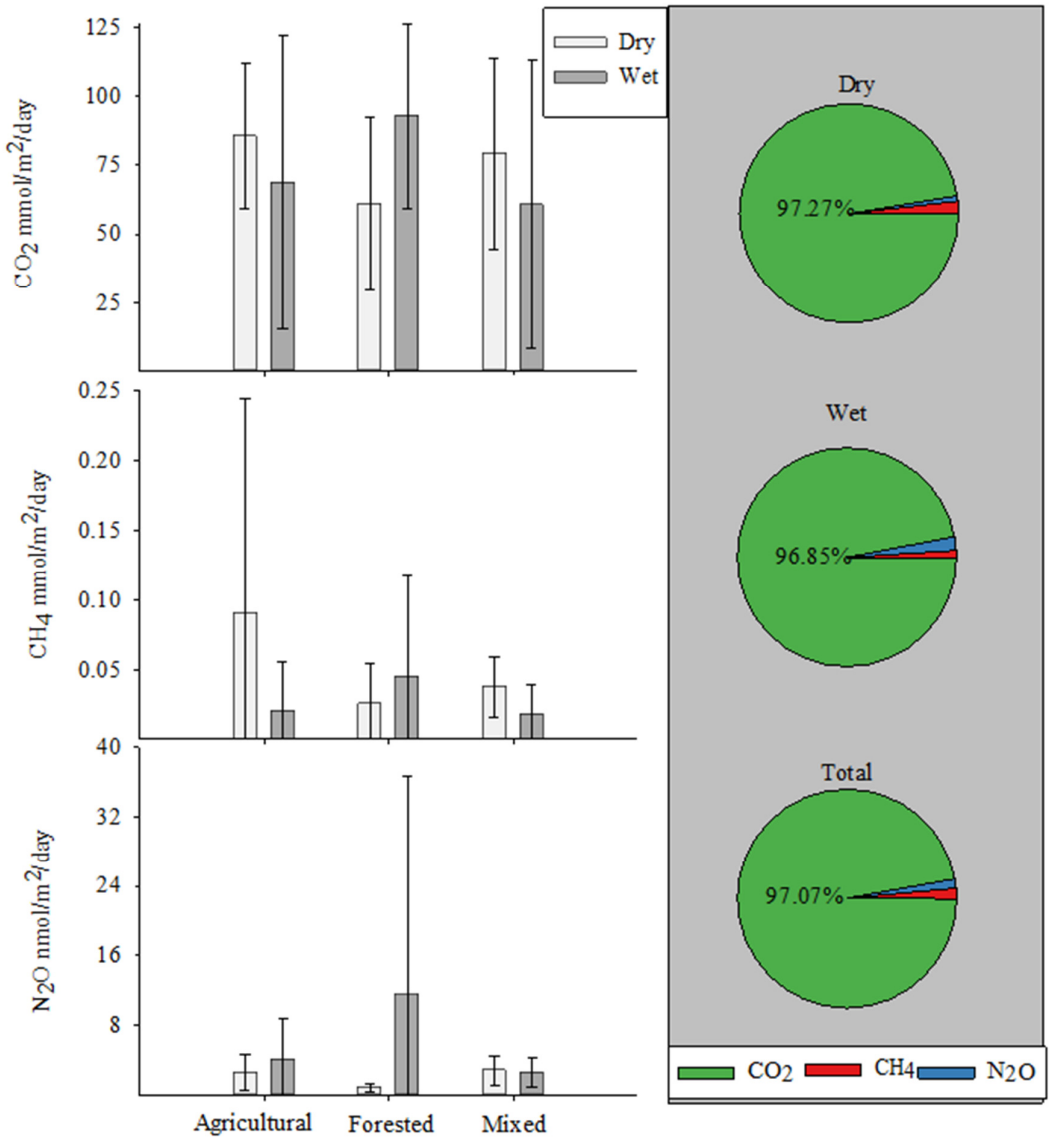

Figure 9. Mean (±SD) fluxes of GHGs from each catchment classification in relation to the hydrology period (left). (Right) The average % contribution of each GHG in relation to total SWGP (20 years) CO_{2eq} emissions (Neubauer and Megonigal, 2015) across all streams.

4. Discussion

Assessing the drivers of GHGs within streams is crucial to developing carbon and nitrogen budgets in rapidly changing catchments. Insights into our original hypotheses were obtained by establishing links between geochemical proxies (DOC, NO_x and DO) and GHGs within streams (Atkins et al., 2017; Stanley et al., 2016; Seitzinger and Kroeze, 1998). Hydrological period impacted geochemical pathways and physical processes that influence GHGs in streams. Groundwater discharge was a not a source of CO_2 and CH_4, but was a contributor to N_2O dynamics. Spatial variations between subtropical streams were attributed to differences in catchment land use following earlier work in temperate systems in the Northern Hemisphere focusing on stream CO_2 (Butman and Raymond, 2011; Hutchins et al., 2019), CH_4 (Stanley et al., 2016; Borges et al., 2018a) and N_2O (Wilcock and Sorrell, 2007; Burgos et al., 2015). Here we discuss the hydrological, geochemical and land-use drivers of GHG and compare our results from subtropical streams to the literature on tropical and temperate streams.

4.1 Hydrological and geochemical drivers of GHG dynamics

Overall, CH_4 and CO_2 showed higher values during the dry than the wet period. Higher CO_2 and CH_4 during low flow (dry) conditions is common across various fluvial settings (Hope et al., 2001). Physical controls over GHG transfer velocities are likely to play an important role in driving this relationship (Raymond et al., 2012). Low flow conditions increase water residence times, therefore reducing instream turbulence limiting gaseous exchange to the atmosphere and promoting the accumulation of GHGs within streams (Webb et al., 2016; Jeffrey et al., 2018; Rocher-Ros et al., 2019). This concept is substantiated CO_2 and CH_4 increased with low DO during the dry period, implying instream respiration and subsequent accumulation of CO_2 and CH_4 in surface waters (Borges et al., 2019; Macklin et al., 2014). During the wet period, increased turbulence and flow has a diluting effect, contributing to the observed decrease in surface water CO_2 and CH_4 (Borges et al., 2018b; Rocher-Ros et al., 2019). Overall, DO and flow regime seem to play a crucial role driving the temporal variability of CH_4 in sub-tropical streams similar to Northern Hemisphere streams.

We also found a negative relationship between DOC and CO_2 during the dry period and a positive relationship during the wet period. The negative correlation during dry conditions supports our interpretation of instream metabolism dominating the CO_2 production pathway during low flow conditions (Marx et al., 2017). However, the positive relationship between

DOC and CO_2 during the wet period suggests an alternate mechanism driving the relationship and might be due to a common source delivery from the soil landscape during runoff events (Hotchkiss et al., 2015). After extended dry periods, flushing events tend to remove accumulated DOC and CO_2 from the soils into streams (Bodmer et al., 2016).

In contrast to CO_2 and CH_4, N_2O significantly increased with runoff and remained relatively constant throughout the dry period. This is likely explained by a combination of 1) direct loading from the soil landscape whereby NOx and N_2O enter streams simultaneously through runoff (Wilcock and Sorrell, 2007), or 2) indirectly through increased availability of DIN facilitating instream N_2O production (Quick et al., 2019). Given the simultaneous occurrence of high CH_4 from low oxygen sediments during the dry period and unlikely suspension of sediment particles due to longer water residence, it is likely that benthic denitrification processes are driving the production of N_2O during the dry period. The source of DIN during dry conditions is typically facilitated through either shallow groundwater or in-stream organic nitrogen (Seitzinger and Kroeze, 1998).

An additional mechanism that can contribute to GHGs dynamics in streams is groundwater discharge, which is commonly neglected in riverine GHGs assessments (Atkins et al., 2017; Drake et al., 2018). During the wet period, we found no significant correlations between the GHGs and radon, probably due to increased surface water connectivity following rain events (Looman et al., 2016a; Atkins et al., 2013). In contrast, N_2O (when outliers removed) displayed positive relationships with radon during the dry period, suggesting that groundwater plays a role in either directly, delivering subsurface waters elevated in higher N_2O, or indirectly, delivering DIN that fuels N_2Oproduction within the stream.

4.2 Influence of land use in driving GHG dynamics

The influence of land use on aquatic CO_2 can be complex and variable. CO_2 increased with forest cover and decreased with mixed modified and agricultural land cover, as previously observed in estuaries in the same area (Looman et al., 2019). The transport of nitrogen from modified catchments to the creek during the wet period can stimulate primary productivity and CO_2 consumption (Borgesa and Gypensb, 2010). Similar to our observations, riverine CO_2 levels were positively influenced by forested biomes in boreal streams in Sweden (Hutchins et al., 2019). Forest soils often have higher rates of soil respiration and OM degradation than agricultural soils (Butman and Raymond, 2011). These processes are enhanced at sub-tropical and tropical latitudes due to higher temperatures as well as greater

terrestrial primary productivity (Butman and Raymond, 2011). In contrast, other studies found higher CO_2 fluxes and concentrations with the forested catchments during the wet period (Bodmer et al., 2016; Borges et al., 2018a), most likely related to adjacent ploughed land where soil disturbance can facilitate higher DOC exports into nearby waterways (Burgos et al., 2015). However, streams assessed in this study were dominated by intensive horticulture which has generally lower levels of soil disturbance (Comer-Warner et al., 2019), potentially limiting DOC and CO_2 fluxes. No relationships were evident between CO_2 and land use during the dry period, possibly as a result of reduced connectivity to the upstream landscape allowing instream processes to mask catchment influences on CO_2 (Webb et al., 2018).

Assessing the influence of land use on CH_4 is challenging given its variability shown across streams and rivers globally (Stanley et al., 2016). Here, in subtropical Australia, CH_4 was positively related with agriculture cover during the dry period. While there is limited direct links between stream CH_4 and agriculture cover (Stanley et al., 2016), previous studies have also found elevated CH_4 associated with agricultural catchments (Borges et al., 2018a). The accumulation of fine sediments in agricultural catchments can cause streambeds to become prone to anoxic conditions, favourable to methanogenesis (Stanley et al., 2016). Here, we demonstrated that the relationship between elevated CH_4 production and agricultural land deteriorated following rainfall events. As described previously, this is likely attributed to shorter water residence time, enhanced oxygenation and dilution compromising methanogenesis (Stanley et al., 2016). Interestingly, moving into the wet period, CH_4 increased with increasing forest cover, which is similar to observations from the Northern Hemisphere (Stanley et al., 2016). Shallow flow paths through the riparian zone which adjoins forest soils rich in OM has previously been suggested to greatly contribute to stream CH_4 concentrations in the US (Jones Jr and Mulholland, 1998) and may explain the findings in our study. In subtropical Australia, while land use may act as an important driver of CH_4 production, episodic rainfall seems to explain most of CH4 dynamics. As opposed to streams in the Northern Hemisphere which are driven by snowmelt and seasonal falls (Crawford et al., 2017; Borges et al., 2018a), hydrology in Australia is driven by episodic rain events.

Spatial variations in N_2O during the dry period were strongly associated with increasing agricultural and mixed modified land cover. Similar to our observations, significantly lower N_2O concentrations were found with increasing forest cover in the tropical Congo (Borges et al., 2019) and Guadalete rivers (Burgos et al., 2015) due to limited application of fertilisers and delivery of DIN from agricultural landscapes. Forested catchments have far lower NO_x

concentrations in comparison to other catchments. NO_x availability has been shown to be an important driver of N_2O in streams in the Northern (Audet et al., 2017; Borges et al., 2018a) and Southern Hemisphere (Wilcock and Sorrell, 2007; Mwanake et al., 2019). A positive relationship between land use and NO_x has been found in Coffs Harbour (White et al., 2018) as well as several other agricultural streams (Beaulieu et al., 2010; Audet et al., 2017; Wilcock and Sorrell, 2007). Interestingly, during the wet period, high NO_x concentrations found within the agricultural catchments did not translate to increased levels of N_2O despite exhibiting a positive linear relationship. This may be related to reduced sub-surface influence caused by increased flow in combination with higher levels of oxygen, which might have compromised denitrification conditions and led to lower N_2O production within the modified and agricultural streams. Alternatively, given that our agricultural sites had relatively lower levels of DOC and high NO_x, conversion of NO_x to N_2O within these sites could have potentially been compromised by carbon limitation (Rosamond et al., 2012).

Despite positive linear correlations during the dry period, DIN is typically transported into stream during periods of rainfall and runoff events (Quick et al., 2019). Given the significant linear correlation between N_2O and radon during the dry, groundwater discharge may be supplying DIN and N_2O to streams within the modified and agricultural catchments (Borges et al., 2019). This process may be driven by the common practice of fertigation in the region (Kaine and Giddings, 2016), which can facilitate groundwater flows rich in nitrogen into streams during dry conditions, potentially contributing to N_2O accumulation. Furthermore, the modification of hydrological pathways through the clearing of vegetation for agriculture can enhance overland flow and groundwater recharge, creating more hydrologically responsive streams (Looman et al., 2019; Petrone, 2010). This means that lower rainfall totals are required to move nitrate and GHGs through the soil horizon, contributing to the higher N_2O fluxes and concentrations seen during the drier period.

4.3 CO_2 CH_4 and N_2O air-water fluxes comparison

We demonstrated that streams in sub-tropical Australia acted as sources of CO_2, CH_4 and N_2O, generating net positive air-water fluxes to the atmosphere. On average, CO_2 fluxes across all catchments and hydrology periods were below the global modelled average for streams (97 – 156 mmol m^{-2} d^{-1}) (Lauerwald et al., 2015). Our measurements were well below other sub-tropical and tropical forest-dominated streams (Borges et al., 2015; de Fátima FL Rasera et al., 2008), as well as agriculture-dominated streams, yet similar to a subtropical

(Yao et al., 2007) and alpine stream with mixed land uses (Qu et al., 2017). Our below average flux estimates for CO_2 may be a reflection of the low piston velocity in sluggish waters that respond primarily to episodic flushing events (Marx et al., 2017).

CH_4 fluxes were highly variable, which is consistent for inland waters (Bastviken et al., 2011), and our estimates fall within the range (4.23 ± 8.41 mmol m^{-2} d^{-1}) for streams and rivers in a recent global meta-analysis (Stanley et al., 2016). However, fluxes were far lower than those reported for agricultural and forested streams in temperate regions of Germany (Bodmer et al., 2016) and African tropical and sub-tropical streams (Borges et al., 2015). Large discrepancies to other studies may be related to our conservative flux estimates as windspeed can be a major driver of piston velocities.N_2O displayed a net-positive flux, which is comparable to that from an alpine stream on the Tibetan plateau in China (Qu et al., 2017), but higher than the forested tributaries of the Mara River in Kenya, and far lower than the modified catchments of the same river (Mwanake et al., 2019). Agricultural streams in midwestern USA, Central Kenya, and Sweden had higher fluxes of N_2O (Beaulieu et al., 2009; Borges et al., 2015; Audet et al., 2017).

Calculating CO_2-equivalent Sustained Global Warming Potentials (SGWP, 20 years) enables us to put in perspective the relative contribution of each GHG given their different levels of potency in the atmosphere (Neubauer and Megonigal, 2015). CO_2 accounted for a vast majority of the CO_2-equivalent emissions (97%), despite being between 250 and 96 times less potent than N_2O and CH_4, respectively (Neubauer and Megonigal, 2015). It is also worth noting that CH_4 had a greater contribution to CO_2 eq emissions during the dry (1.94 % dry versus 1.11 % wet), while N_2O had a greater contribution during the wet (2.01 % wet versus 0.78 % dry) (Fig. 9). The difference in % contribution between N_2O and CH_4 in relation to the hydrological phase highlights that hydrology can play a crucial role in driving GHGs and, accounting for this may improve current uncertainties in global models and budgets.

4.4 Conclusion

The present study demonstrated that streams in subtropical Australia acted as sources of CO_2, CH_4, and N_2O, generating net positive air-water fluxes to the atmosphere. This is consistent to findings in the Northern Hemisphere, yet emissions rates for CO_2 tended to be lower than the global average. Further, we found that the episodic wet climate in sub-tropical Australia drove changes in stream GHGs through the release of soil NO_X and DOC following rainfall events. Groundwater discharge as traced by radon was not a source of CO_2 and CH_4, but seemed to influence N_2O dynamics. CO_2 and CH_4 increased with catchment forest cover during the wet

period, while N_2O and CH_4 increased with agricultural catchment area during the dry period. Overall, this study shows how DOC and NO_X, land-use, and rainfall events interact to drive spatial and temporal dynamics in stream greenhouse gases in sub-tropical streams. These findings have implications for improving current global outgassing estimations of GHGs in sub-tropical wet-dry climates. Further, it highlights the need to account for the influence of anthropogenic perturbation on GHG dynamics in streams.

Reference List

Atkins ML, Santos IR and Maher DT. (2017) Seasonal exports and drivers of dissolved inorganic and organic carbon, carbon dioxide, methane and delta(13)C signatures in a subtropical river network. *Sci Total Environ* 575: 545-563.

Atkins ML, Santos IR, Ruiz-Halpern S, et al. (2013) Carbon dioxide dynamics driven by groundwater discharge in a coastal floodplain creek. *Journal of Hydrology* 493: 30-42.

Audet J, Wallin MB, Kyllmar K, et al. (2017) Nitrous oxide emissions from streams in a Swedish agricultural catchment. *Agriculture, Ecosystems & Environment* 236: 295-303.

Aufdenkampe AK, Mayorga E, Raymond PA, et al. (2011) Riverine coupling of biogeochemical cycles between land, oceans, and atmosphere. *Frontiers in Ecology and the Environment* 9: 53-60.

Australian Government Bureau of Meteorology (2019a). *Monthly climate statistics for Coffs Harbour weather station, NSW.* Retrieved from http://www.bom.gov.au/climate/averages/

Australian Bureau of Meteorology (2019b). *Australian Landscape Water Balance* [Dataset] Available at: http://www.bom.gov.au/water/landscape/

Bass AM, Bird MI, Liddell MJ, et al. (2011) Fluvial dynamics of dissolved and particulate organic carbon during periodic discharge events in a steep tropical rainforest catchment. *Limnology and Oceanography* 56.

Bass AM, Munksgaard NC, Leblanc M, et al. (2014) Contrasting carbon export dynamics of human impacted and pristine tropical catchments in response to a short-lived discharge event. *Hydrological Processes* 28: 1835-1843.

Bastviken D, Tranvik LJ, Downing JA, et al. (2011) Freshwater methane emissions offset the continental carbon sink. *Science* 331: 50.

Beaulieu J, Arango C and Tank J. (2009) The effects of season and agriculture on nitrous oxide production in headwater streams. *Journal of Environmental Quality* 38: 637-646.

Beaulieu J, Shuster W and Rebholz J. (2010) Nitrous oxide emissions from a large, impounded river: The Ohio River. *Environmental science technology* 44: 7527-7533.

Bodmer P, Heinz M, Pusch M, et al. (2016) Carbon dynamics and their link to dissolved organic matter quality across contrasting stream ecosystems. *Sci Total Environ* 553: 574-586.

Borges, Darchambeau F, Lambert T, et al. (2018a) Effects of agricultural land use on fluvial carbon dioxide, methane and nitrous oxide concentrations in a large European river, the Meuse (Belgium). *Sci Total Environ* 610-611: 342-355.

Borges AV, Abril G and Bouillon S. (2018b) Carbon dynamics and CO2 and CH4 outgassing in the Mekong delta. *Biogeosciences* 15: 1093-1114.

Borges AV, Darchambeau F, Lambert T, et al. (2019) Variations in dissolved greenhouse gases (CO2, CH4, N2O) in the Congo River network overwhelmingly driven by fluvial-wetland connectivity. *Biogeosciences* 16: 3801-3834.

Borges AV, Darchambeau F, Teodoru CR, et al. (2015) Globally significant greenhouse-gas emissions from African inland waters. *Nature Geoscience* 8: 637-642.

Borges AV, Vanderborght J-P, Schiettecatte L-S, et al. (2004) Variability of the gas transfer velocity of CO2 in a macrotidal estuary (the Scheldt). *Estuaries* 27: 593-603.

Borges AV and Gypensb N. (2010) Carbonate chemistry in the coastal zone responds more strongly to eutrophication than ocean acidification. *Limnology and Oceanography* 55: 346-353.

Burgos M, Sierra A, Ortega T, et al. (2015) Anthropogenic effects on greenhouse gas (CH4 and N2O) emissions in the Guadalete River Estuary (SW Spain). *Sci Total Environ* 503-504: 179-189.

Burnett WC, Kim G and Lane-Smith D. (2001) A continuous monitor for assessment of 222Rn in the coastal ocean. *Journal of Radioanalytical and Nuclear Chemistry* 249: 167-172.

Butman D and Raymond PA. (2011) Significant efflux of carbon dioxide from streams and rivers in the United States. *Nature Geoscience* 4: 839-842.

Canfield DE, Glazer AN and Falkowski PG. (2010) The evolution and future of Earth's nitrogen cycle. *science* 330: 192-196.

Coffs Harbour City Council (2012). *Coffs Harbour Biodiversity Action Strategy: From the Oceans to the Ranges*. *Part B: The Landscapes of Coffs Harbour*. Coffs Harbour City Council, NSW. Retreived from http://www.coffsharbour.nsw.gov.au/our-environment/Documents/Biodiversity%20Action%20Strategy_PART%20B_August%202012

Cole JJ, Prairie YT, Caraco NF, et al. (2007) Plumbing the Global Carbon Cycle: Integrating Inland Waters into the Terrestrial Carbon Budget. *Ecosystems* 10: 172-185.

Comer-Warner SA, Gooddy DC, Ullah S, et al. (2019) Seasonal variability of sediment controls of carbon cycling in an agricultural stream. *Science of the Total Environment* 688: 732-741.

Conrad SR, Santos IR, Brown DR, et al. (2017) Mangrove sediments reveal records of development during the previous century (Coffs Creek estuary, Australia). *Mar Pollut Bull* 122: 441-445.

Crawford JT, Loken LC, West WE, et al. (2017) Spatial heterogeneity of within-stream methane concentrations. *Journal of Geophysical Research: Biogeosciences* 122: 1036-1048.

De Fátima FL Rasera M, Ballester MVR, Krusche AV, et al. (2008) Estimating the surface area of small rivers in the southwestern Amazon and their role in CO2 outgassing. *Earth Interactions* 12: 1-16.

Dinsmore KJ, Wallin MB, Johnson MS, et al. (2013) Contrasting CO2concentration discharge dynamics in headwater streams: A multi-catchment comparison. *Journal of Geophysical Research: Biogeosciences* 118: 445-461.

Drake TW, Raymond PA and Spencer RGM. (2018) Terrestrial carbon inputs to inland waters: A current synthesis of estimates and uncertainty. *Limnology and Oceanography Letters* 3: 132-142.

Hope D, Palmer SM, Billett MF, et al. (2001) Carbon dioxide and methane evasion from a temperate peatland stream. *Limnology and Oceanography* 46.

Hotchkiss ER, Hall Jr RO, Sponseller RA, et al. (2015) Sources of and processes controlling CO2 emissions change with the size of streams and rivers. *Nature Geoscience* 8: 696-699.

Hutchins RH, Prairie YT and del Giorgio PA. (2019) Large-Scale Landscape Drivers of CO2, CH4, DOC, and DIC in Boreal River Networks. *Global Biogeochemical Cycles* 33: 125-142.

Jeffrey LC, Maher DT, Santos IR, et al. (2018) The spatial and temporal drivers of pCO2, pCH4 and gas transfer velocity within a subtropical estuary. *Estuarine, Coastal and Shelf Science* 208: 83-95.

Jones Jr JB and Mulholland PJ. (1998) Methane input and evasion in a hardwood forest stream: Effects of subsurface flow from shallow and deep pathway. *Limnology and Oceanography* 43: 1243-1250.

Kaine G and Giddings J. (2016) Erosion control, irrigation and fertiliser management and blueberry production: Grower interviews. Hauturu, New Zealand: Report to Coffs Harbour Landcare.

Lauerwald R, Laruelle GG, Hartmann J, et al. (2015) Spatial patterns in CO2 evasion from the global river network. *Global Biogeochemical Cycles* 29: 534-554.

Lee J-M and Kim G. (2006) A simple and rapid method for analyzing radon in coastal and ground waters using a radon-in-air monitor. *Journal of Environmental Radioactivity* 89: 219-228.

Looman A, Maher DT, Pendall E, et al. (2016a) The carbon dioxide evasion cycle of an intermittent first-order stream: contrasting water–air and soil–air exchange. *Biogeochemistry* 132: 87-102.

Looman A, Santos IR, Tait DR, et al. (2019) Dissolved carbon, greenhouse gases, and δ13C dynamics in four estuaries across a land use gradient. *Aquatic Sciences* 81.

Looman A, Santos IR, Tait DR, et al. (2016b) Carbon cycling and exports over diel and flood-recovery timescales in a subtropical rainforest headwater stream. *Sci Total Environ* 550: 645-657.

Maavara T, Lauerwald R, Laruelle GG, et al. (2019) Nitrous oxide emissions from inland waters: Are IPCC estimates too high? *Glob Chang Biol* 25: 473-488.

MacDonald LH and Coe D. (2007) Influence of headwater streams on downstream reaches in forested areas. *Forest Science* 53: 148-168.

Macklin PA, Maher DT and Santos IR. (2014) Estuarine canal estate waters: Hotspots of CO2 outgassing driven by enhanced groundwater discharge? *Marine Chemistry* 167: 82-92.
Maher DT, Call M, Macklin P, et al. (2019) Hydrological Versus Biological Drivers of Nutrient and Carbon Dioxide Dynamics in a Coastal Lagoon. *Estuaries and Coasts* 42: 1015-1031.
Marx A, Dusek J, Jankovec J, et al. (2017) A review of CO2 and associated carbon dynamics in headwater streams: A global perspective. *Reviews of Geophysics* 55: 560-585.
Marzadri A, Dee MM, Tonina D, et al. (2017) Role of surface and subsurface processes in scaling N2O emissions along riverine networks. *Proceedings of the National Academy of Sciences* 114: 4330-4335.
Milford H. (1999) *Soil Landscapes of the Coffs Harbour: 1: 100 000 Sheet (Athol Glen, Corindi Beach, Urunga, Coramba)*: Department of Land and Water Conservation.
Mwanake R, Gettel G, Aho K, et al. (2019) Land use, not stream order, controls N2O concentration and flux in the upper Mara River basin, Kenya. *Journal of Geophysical Research: Biogeosciences*.
Neubauer SC and Megonigal JP. (2015) Moving Beyond Global Warming Potentials to Quantify the Climatic Role of Ecosystems. *Ecosystems* 18: 1000-1013.
Parliamentary Counsel's Office. (2013) Coffs Harbour Local Environmental Plan NSW Government.
Petrone KC. (2010) Catchment export of carbon, nitrogen, and phosphorus across an agro-urban land use gradient, Swan-Canning River system, southwestern Australia. *Journal of Geophysical Research* 115.
Petrone KC, Fellman JB, Hood E, et al. (2011) The origin and function of dissolved organic matter in agro-urban coastal streams. *Journal of Geophysical Research* 116.
Petrone KC, Richards JS and Grierson PF. (2008) Bioavailability and composition of dissolved organic carbon and nitrogen in a near coastal catchment of south-western Australia. *Biogeochemistry* 92: 27-40.
Pierrot D, Neill C, Sullivan K, et al. (2009) Recommendations for autonomous underway pCO2 measuring systems and data-reduction routines. *Deep Sea Research Part II: Topical Studies in Oceanography* 56: 512-522.
Qu B, Aho KS, Li C, et al. (2017) Greenhouse gases emissions in rivers of the Tibetan Plateau. *Scientific reports* 7: 1-8.
Quick AM, Reeder WJ, Farrell TB, et al. (2019) Nitrous oxide from streams and rivers: A review of primary biogeochemical pathways and environmental variables. *Earth-science reviews* 191: 224-262.
Raymond P and Cole J. (2001) Gas exchange in rivers and estuaries: Choosing a gas transfer velocity. *Estuaries* 24: 312-317.
Raymond PA, Zappa CJ, Butman D, et al. (2012) Scaling the gas transfer velocity and hydraulic geometry in streams and small rivers. *Limnology and Oceanography: Fluids and Environments* 2: 41-53.
Rocher-Ros G, Sponseller RA, Lidberg W, et al. (2019) Landscape process domains drive patterns of CO2 evasion from river networks. *Limnology and Oceanography Letters* 4: 87-95.
Rosamond MS, Thuss SJ and Schiff SL. (2012) Dependence of riverine nitrous oxide emissions on dissolved oxygen levels. *Nature geoscience* 5: 715.
Sadat-Noori M, Maher DT and Santos IR. (2015) Groundwater Discharge as a Source of Dissolved Carbon and Greenhouse Gases in a Subtropical Estuary. *Estuaries and Coasts* 39: 639-656.
Sawakuchi HO, Neu V, Ward ND, et al. (2017) Carbon Dioxide Emissions along the Lower Amazon River. *Frontiers in Marine Science* 4.
Seitzinger S, Mayorga E, Bouwman A, et al. (2010) Global river nutrient export: A scenario analysis of past and future trends. *Global Biogeochemical Cycles* 24.
Seitzinger SP and Kroeze C. (1998) Global distribution of nitrous oxide production and N inputs in freshwater and coastal marine ecosystems. *Global biogeochemical cycles* 12: 93-113.
Smith RM and Kaushal SS. (2015) Carbon cycle of an urban watershed: exports, sources, and metabolism. *Biogeochemistry* 126: 173-195.

Stanley EH, Casson NJ, Christel ST, et al. (2016) The ecology of methane in streams and rivers: patterns, controls, and global significance. *Ecological Monographs* 86: 146-171.
Wanninkhof R. (1992) Relationship between wind speed and gas exchange over the ocean. *Journal of Geophysical Research: Oceans* 97.
Webb JR, Santos IR, Maher DT, et al. (2018) The Importance of Aquatic Carbon Fluxes in Net Ecosystem Carbon Budgets: A Catchment-Scale Review. *Ecosystems* 22: 508-527.
Webb JR, Santos IR, Tait DR, et al. (2016) Divergent drivers of carbon dioxide and methane dynamics in an agricultural coastal floodplain: Post-flood hydrological and biological drivers. *Chemical Geology* 440: 313-325.
Weiss RF and Price BA. (1980) Nitrous oxide solubility in water and seawater. *Marine Chemistry* 8.
White SA, Santos IR and Hessey S. (2018) Nitrate loads in sub-tropical headwater streams driven by intensive horticulture. *Environ Pollut* 243: 1036-1046.
Wilcock RJ and Sorrell BK. (2007) Emissions of Greenhouse Gases CH4 and N2O from Low-gradient Streams in Agriculturally Developed Catchments. *Water, Air, and Soil Pollution* 188: 155-170.
Yamamoto S, Alcauskas JB and Crozier TE. (1976) Solubility of methane in distilled water and seawater. *Journal of Chemical & Engineering Data* 21: 78-80.
Yao G, Gao Q, Wang Z, et al. (2007) Dynamics of CO2 partial pressure and CO2 outgassing in the lower reaches of the Xijiang River, a subtropical monsoon river in China. *Science of the Total Environment* 376: 255-266.

Appendices

Appendix A1

Table A1. Pearson correlation matrix summary for % catchment land use (left) and DO, DOC, NO_x (right) versus greenhouse gas concentrations during the dry (n=84) and wet (n=77) periods. Values in bold denote significance at the 0.05 level (2-tailed).

Hydrology period	Catchment Landuse	CO_2	CH_4	N_2O	Physicochemical Parameters	CO_2	CH_4	N_2O
Dry	Agriculture (%)	r^2=0.023	r^2=0.23	r^2=0.22	DO (%sat)	r^2=0.31	r^2=0.27	r^2=0.15
		p=0.83	**p=0.03***	**p=0.04***		**p<0.01***	**p=0.01***	p=0.16
	Forest (%)	r^2=-0.08	r^2=-0.16	r^2=-0.46	NO_x (µmol L^{-1})	r^2=-0.11	r^2=-0.14	r^2=0.70
		p=**0.44**	p=0.13	p**<0.01***		p=0.28	p=0.19	p**<0.01***
	Mixed Modified (%)	r^2=0.08	r^2=0.16	r^2=0.46	DOC (µmol L^{-1})	r^2=-0.23	r^2=-0.0	r^2=-0.16
		p=0.44	p=0.13	p=0.13		**p=0.03***	p=0.39	p=0.13
Wet	Agriculture (%)	r^2=-0.45	r^2=-0.20	r^2=-0.07	DO (%sat)	r^2=-0.70	r^2=-0.60	r^2=0.040
		p<0.01*	p=0.05	p=0.49		**p<0.01***	**p<0.01***	p=0.73
	Forest (%)	r^2=0.46	r^2=0.23	r^2=0.18	NO_x (µmol L^{-1})	r^2=-0.22	r^2=-215	r^2=0.65
		p<0.01*	**p=0.04***	p=0.10		p=0.05	p=0.05	**p<0.01***
	Mixed Modified (%)	r^2=-0.46	r^2=-0.23	r^2=-0.18	DOC (µmol L^{-1})	r^2=0.26	r^2=0.20	r^2=0.24
		p<0.01*	**p=0.04***	p=0.10		**p=0.02***	p=0.08	**p=0.03***

Appendix B1

Table B1. Raw data summary. Fluxes calculated from 0 km hr^{-1} windspeed and derived from (Borges, 2004). CO_{2eq} listed as percentages derived from calculations from (Neubauer and Megonigal, 2015).

Site	Sample	CO_2 mmol m^{-2} d^{-1}	CH_4 mmol m^{-2} d^{-1}	N_2O umol m^{-2} d^{-1}	CO_{2eq}	CH_4 (CO_{2eq})	N_2O (CO_{2eq})	CO_2 (%sat)	N_2O (%sat)	CH_4 (% sat)	Temp (°C)	pH	DO (%)	NO_X (umol/L)	DOC (umol/L)
Arrawarra creek	1	63.27	0.01	1.86	99	0.4	0.8	1150.8	147.3	690.0	24.6	7.10	48	3.43	536.89
Arrawarra creek	2	30.76	0.01	0.99	98	0.8	0.8	474.0	120.1	598.0	22.4	7.01	2	0.79	1502.08
Arrawarra creek	3	24.14	0.01	0.99	97	1.8	1.0	571.6	126.1	1280.4	28.3	7.32	69	1.29	1054.02
Arrawarra creek	4	41.41	0.00	1.18	99	0.3	0.7	905.2	128.0	405.8	30.6	7.13	46	2.43	932.25
Arrawarra creek	5	57.34	0.00	2.32	99	0.2	1.0	1180.9	158.8	376.0	28.7	6.71	55	4.36	369.38
Arrawarra creek	6	31.59	0.00	1.01	99	0.2	0.8	675.0	128.1	250.6	25.0	7.00	50	1.64	564.08
Arrawarra creek	7	82.89	0.01	2.10	99	0.2	0.7	1453.1	157.6	627.9	21.9	6.70	40	4.14	354.31
Arrawarra creek	8	55.83	0.00	1.22	99	0.2	0.6	1036.0	133.5	451.6	22.8	6.84	57	1.71	395.86
Arrawarra creek	9	57.57	0.00	1.25	99	0.1	0.6	1103.9	134.0	268.0	24.6	6.96	28	0.64	447.73
Arrawarra creek	10	148.66	0.01	2.15	99	0.2	0.4	2597.8	154.6	818.0	25.8	6.91	45	2.36	410.51
Arrawarra creek	11	94.27	0.02	2.16	99	0.7	0.6	1620.5	156.5	1783.7	23.3	6.89	37	5.00	433.20
Arrawarra creek	12	73.59	0.01	4.00	98	0.3	1.4	1179.6	198.0	685.0	22.3	7.04	65	6.86	348.52
Arrawarra creek	13	58.05	0.01	-0.12	100	0.3	-0.1	1164.3	96.8	614.0	27.5	7.11	51	2.64	295.40
Arrawarra creek	14	58.47	0.01	1.59	99	0.6	0.7	1036.8	142.9	996.8	21.8	7.70	58	4.43	269.97
Arrawarra creek	15	67.93	0.00	5.69	98	0.2	2.1	1126.2	239.8	490.3	23.3	8.09	72	9.50	319.84
Boambee creek	2	106.32	0.02	4.07	98	0.6	1.1	1306.2	175.5	1333.1	22.6	6.88	58	9.20	183.86
Boambee creek	3	75.36	0.02	4.60	98	0.9	1.6	1159.7	207.3	1586.8	22.6	6.48	40	4.86	99.37
Boambee creek	4	130.30	0.04	0.36	99	1.0	0.1	1803.3	107.4	2717.8	25.4	6.75	46	5.21	186.17
Boambee creek	5	128.28	0.03	6.11	98	0.8	1.2	1610.4	219.1	1960.2	22.8	6.66	29	6.14	130.84
Boambee creek	6	110.19	0.03	5.06	98	0.9	1.2	1621.1	211.9	2203.7	24.1	6.58	35	5.50	225.38

Boambee creek	7	118.24	0.02	3.76	99	0.5	0.8	1453.8	171.5	1179.1	22.7	6.69	48	6.00	100.08
Boambee creek	8	144.40	0.01	5.59	99	0.4	1.0	1762.8	207.6	1063.1	22.3	6.67	49	2.86	150.32
Boambee creek	9	152.06	0.03	5.54	98	0.8	0.9	1952.3	208.8	2320.2	24.1	6.60	33	2.50	110.03
Boambee creek	10	269.74	0.05	4.95	99	0.6	0.5	2754.4	180.9	2847.5	22.8	6.60	41	5.00	122.02
Boambee creek	11	67.64	0.00	3.93	98	0.2	1.5	778.8	166.4	362.0	22.0	6.86	84	23.64	175.64
Boambee creek	12	83.66	0.02	7.65	97	0.9	2.3	811.8	211.2	1206.2	21.0	7.11	87	30.64	239.08
Boambee creek	13	51.36	0.00	2.37	99	0.3	1.2	710.8	147.0	361.1	22.5	7.02	80	6.79	231.50
Boambee creek	14	53.28	0.00	2.47	99	0.3	1.2	687.1	146.1	362.2	21.5	7.36	80	6.07	266.40
Boambee creek	15	62.04	0.00	3.18	98	0.2	1.3	626.4	145.6	278.0	21.8	8.05	86	15.21	310.89
Bonville creek	2	48.13	0.02	1.63	98	1.0	1.1	672.3	132.5	1147.8	22.0	6.86	74	3.85	145.58
Bonville creek	3	8.48	0.00	1.24	96	0.1	3.7	233.1	129.7	118.4	25.5	6.48	63	1.64	131.92
Bonville creek	4	75.77	0.05	2.70	97	2.1	0.9	1096.5	157.4	3485.5	23.8	6.73	57	2.43	146.08
Bonville creek	5	62.36	0.02	2.24	98	1.1	0.9	886.5	146.4	1475.1	23.2	6.60	61	2.57	168.72
Bonville creek	6	52.63	0.02	1.75	98	1.0	0.9	852.3	140.2	1291.2	23.8	6.64	61	2.93	117.48
Bonville creek	7	60.39	0.02	1.95	98	0.9	0.8	806.1	138.7	1170.6	21.5	6.68	66	1.93	121.35
Bonville creek	8	73.09	0.01	2.68	98	0.7	0.9	1002.6	154.8	1100.2	22.7	6.53	63	2.36	146.83
Bonville creek	9	63.80	0.03	-0.09	98	1.8	0.0	892.6	98.2	2458.0	22.9	6.60	64	1.93	98.29
Bonville creek	10	71.35	0.02	1.57	99	0.8	0.6	831.4	127.1	1017.1	22.0	6.66	86	10.43	105.24
Bonville creek	11	41.24	0.01	1.45	98	1.1	0.9	559.1	127.5	907.7	21.4	6.84	81	4.50	88.13
Bonville creek	12	40.04	0.01	1.57	98	0.7	1.0	471.7	125.4	515.4	19.9	6.97	85	3.50	253.57
Bonville creek	13	30.82	0.01	1.14	97	1.6	0.9	478.0	124.2	1117.8	20.7	6.88	84	3.07	126.68
Bonville creek	14	29.74	0.01	1.40	98	0.8	1.2	442.0	128.2	541.9	19.9	7.73	88	2.79	140.90
Bonville creek	15	34.78	0.01	1.78	98	0.5	1.3	421.5	128.3	396.6	20.6	7.65	88	10.64	232.29
Coffs creek	1	83.55	0.05	2.96	97	2.0	1.0	992.8	148.8	3060.8	23.8	7.01	46	11.24	328.33

Coffs creek	2	77.84	0.06	1.81	97	2.6	0.6	1074.7	134.3	3940.6	27.0	7.02	24	1.57	339.57
Coffs creek	3	96.88	0.09	2.15	96	3.0	0.6	1548.1	146.2	6435.4	27.9	6.77	13	0.07	302.56
Coffs creek	4	85.73	0.07	3.51	96	2.7	1.0	1171.9	165.4	4362.6	27.5	6.94	27	3.21	594.26
Coffs creek	5	88.84	0.07	6.30	96	2.5	1.8	1026.7	209.3	3867.2	22.7	6.70	30	10.79	407.39
Coffs creek	6	85.33	0.05	3.82	97	1.9	1.1	1232.5	178.1	3481.2	25.9	6.70	39	4.29	510.38
Coffs creek	7	90.10	0.05	1.32	98	1.7	0.4	1028.4	122.4	2692.2	23.2	6.75	35	0.93	240.95
Coffs creek	8	108.30	0.07	1.19	97	2.3	0.3	1240.3	120.7	4328.3	23.2	6.72	10	0.00	299.98
Coffs creek	9	111.91	0.08	0.79	97	2.4	0.2	1349.6	114.1	4692.9	25.0	6.82	17	0.29	241.62
Coffs creek	10	179.10	0.08	3.79	98	1.6	0.5	1672.7	154.7	4102.5	23.8	6.88	37	5.71	255.19
Coffs creek	11	78.34	0.03	4.93	97	1.1	1.6	787.6	172.5	1385.4	22.3	6.86	61	19.57	384.07
Coffs creek	12	64.33	0.02	6.29	96	1.3	2.5	582.6	180.3	1132.1	21.2	7.09	76	62.29	354.60
Coffs creek	13	43.48	0.03	1.73	97	2.1	1.0	558.2	130.8	1684.5	21.7	6.83	86	9.57	163.10
Coffs creek	14	42.65	0.03	1.95	97	2.3	1.2	536.0	133.2	1735.2	22.5	7.91	85	8.29	297.28
Coffs creek	15	55.40	0.02	2.80	97	1.3	1.3	523.3	136.5	1033.5	21.2	7.95	68	27.71	323.34
Cordwell creek	2	97.79	0.14	1.30	95	4.3	0.4	1127.7	121.1	9448.6	22.4	6.84	35	3.13	212.70
Cordwell creek	3	114.71	0.69	0.86	83	17.3	0.2	1772.2	119.2	52199.6	25.9	6.49	4	0.07	203.57
Cordwell creek	4	118.48	0.21	0.40	94	5.7	0.1	1494.6	107.7	13128.8	24.3	6.82	10	0.07	209.06
Cordwell creek	5	79.14	0.14	0.54	94	5.8	0.2	1018.1	110.0	8767.2	24.8	6.81	13	0.00	222.22
Cordwell creek	6	93.43	0.30	1.03	90	9.9	0.3	1292.7	121.5	20779.0	23.5	6.58	56	0.43	219.39
Cordwell creek	7	113.87	0.02	0.60	99	0.5	0.1	1248.5	110.3	1116.6	21.4	6.65	27	0.00	225.30
Cordwell creek	8	99.47	0.26	0.89	92	8.2	0.2	1160.4	115.9	15270.7	22.4	6.90	45	0.14	204.65
Cordwell creek	9	120.12	0.08	0.59	98	2.2	0.1	1419.3	110.6	4699.0	23.3	6.46	5	0.36	343.24
Cordwell creek	10	240.03	0.16	1.07	98	2.3	0.1	2166.4	115.4	7886.5	22.0	6.57	8	0.00	199.36
Cordwell creek	11	128.90	0.05	4.43	98	1.4	0.9	1281.1	169.2	2820.7	21.1	6.62	31	2.43	267.14

Cordwell creek	12	75.26	0.00	4.29	98	0.2	1.5	695.8	158.0	252.1	20.9	6.80	58	30.36	270.72
Cordwell creek	13	48.50	0.02	0.83	98	1.2	0.4	619.7	115.4	1117.6	20.8	6.85	91	2.14	120.14
Cordwell creek	14	55.82	0.03	0.90	98	2.0	0.4	664.0	115.7	1970.7	20.5	7.98	39	1.64	142.90
Cordwell creek	15	32.99	0.03	0.86	96	2.9	0.7	357.2	111.4	1356.0	21.4	7.32	68	4.71	200.49
Corindi creek	1	58.02	0.04	0.69	98	2.0	0.4	896.1	114.9	3124.1	25.2	6.94	45	0.21	364.38
Corindi creek	2	73.71	0.03	0.67	98	1.4	0.2	1211.8	115.7	2458.0	25.3	6.75	28	0.86	317.76
Corindi creek	3	33.54	0.02	0.93	97	2.2	0.7	713.6	121.2	1903.1	30.5	6.90	56	0.00	389.74
Corindi creek	4	41.72	0.01	0.45	99	1.0	0.3	776.8	110.2	1082.8	28.7	7.02	43	0.29	371.29
Corindi creek	5	49.68	0.03	0.87	98	1.9	0.4	862.9	119.7	2215.7	27.0	6.88	58	0.64	372.75
Corindi creek	6	28.37	0.01	0.43	98	1.3	0.4	574.6	110.2	964.7	27.4	7.09	54	0.50	405.35
Corindi creek	7	53.19	0.07	0.61	95	4.3	0.3	830.0	113.6	5241.0	23.3	6.80	7	0.00	358.14
Corindi creek	8	19.55	0.00	1.26	98	0.6	1.6	380.8	128.5	369.4	24.5	6.96	31	0.00	351.64
Corindi creek	9	50.39	0.01	0.62	99	0.6	0.3	852.0	114.0	758.9	26.0	6.90	168	0.07	376.71
Corindi creek	10	110.13	0.04	0.10	99	1.4	0.0	1565.4	102.1	3111.2	26.3	6.91	23	0.00	308.81
Corindi creek	11	56.37	0.02	0.57	98	1.5	0.3	843.7	111.9	1786.3	24.8	7.01	31	0.00	313.55
Corindi creek	12	111.46	0.33	1.02	91	9.3	0.2	1321.0	118.5	19872.6	23.0	6.81	8	0.00	333.54
Corindi creek	13	65.97	0.02	0.55	99	1.1	0.2	992.7	112.3	1643.9	22.7	6.42	24	0.14	305.00
Corindi creek	14	69.13	0.03	0.49	98	1.6	0.2	989.9	110.7	2422.5	21.5	7.27	19	0.00	552.34
Corindi creek	15	64.38	0.03	1.14	98	1.8	0.5	893.8	121.4	2288.5	26.8	7.50	55	0.00	399.94
Ferntree Creek	1	43.70	0.03	2.37	97	2.0	1.4	704.3	151.6	2266.4	24.0	7.12	53	16.29	273.75
Ferntree Creek	2	47.26	0.04	3.13	96	2.7	1.7	813.5	171.9	3124.5	25.9	6.99	29	13.86	216.18
Ferntree Creek	3	49.09	0.06	3.74	94	3.7	1.9	962.0	190.8	4794.1	28.3	6.84	31	16.43	317.38
Ferntree Creek	4	56.32	0.05	2.55	96	2.8	1.1	986.8	157.3	3737.1	27.9	6.95	30	6.64	507.63
Ferntree Creek	5	43.36	0.05	2.24	95	3.8	1.3	701.6	150.5	3885.2	23.4	6.89	43	7.43	425.87

Ferntree Creek	6	32.09	0.02	3.04	96	1.8	2.4	652.1	173.4	1572.6	27.9	6.92	51	14.14	513.13
Ferntree Creek	7	43.65	0.03	2.29	97	2.1	1.3	721.2	152.7	2163.6	23.6	6.90	4	9.86	323.46
Ferntree Creek	8	47.81	0.02	3.04	97	1.7	1.6	754.9	168.3	1882.5	23.1	6.97	34	9.00	260.93
Ferntree Creek	9	55.34	0.03	1.86	97	2.1	0.9	870.5	141.6	2656.5	23.9	6.92	34	5.29	263.06
Ferntree Creek	10	113.70	0.08	5.01	96	2.4	1.1	1584.3	201.6	5681.9	25.6	6.65	35	12.14	213.98
Ferntree Creek	11	43.12	0.02	2.46	97	1.2	1.4	625.5	150.3	1185.7	22.1	6.97	59	31.29	223.18
Ferntree Creek	12	33.39	0.01	2.36	97	0.9	1.8	432.0	140.3	634.0	20.6	7.30	79	35.93	193.83
Ferntree Creek	13	20.24	0.01	1.28	97	1.3	1.6	358.0	128.0	690.4	21.0	6.98	92	24.64	111.98
Ferntree Creek	14	20.93	0.01	0.17	98	1.5	0.2	370.9	103.7	747.8	22.9	7.94	98	18.29	186.58
Ferntree Creek	15	30.47	0.01	1.44	98	1.0	1.2	398.0	124.0	617.6	21.2	8.11	86	19.21	148.24
Hearnes lake	1	55.63	0.01	4.03	97	0.4	2.1	599.5	153.3	427.8	24.1	7.18	60	59.72	264.03
Hearnes lake	2	46.46	0.01	2.05	98	0.7	1.1	522.1	130.5	589.6	23.9	7.24	46	9.21	213.68
Hearnes lake	3	52.85	0.01	1.11	99	0.6	0.5	769.5	121.0	697.6	27.3	7.03	45	1.21	244.16
Hearnes lake	4	63.42	0.01	1.17	99	0.4	0.5	771.3	118.3	460.7	28.7	7.13	56	0.14	349.56
Hearnes lake	5	51.81	0.01	1.77	98	0.7	0.9	583.7	126.0	595.0	26.1	7.07	54	1.43	221.14
Hearnes lake	6	42.79	0.01	0.96	99	0.5	0.6	570.0	116.6	484.3	25.6	7.12	53	1.14	248.90
Hearnes lake	7	79.69	0.02	1.31	99	1.1	0.4	826.8	119.5	1322.4	24.1	6.50	9	0.50	292.45
Hearnes lake	8	56.62	0.00	2.16	99	0.3	1.0	616.2	132.5	309.9	23.4	7.07	48	3.64	185.88
Hearnes lake	9	61.35	0.00	2.56	99	0.2	1.1	675.4	139.1	322.1	24.2	6.97	49	4.57	173.55
Hearnes lake	10	125.12	0.01	5.00	99	0.2	1.0	1026.6	162.1	446.5	22.4	6.95	84	10.64	174.93
Hearnes lake	11	67.28	0.00	1.74	99	0.2	0.7	677.6	125.0	297.2	22.6	6.95	52	3.43	175.59
Hearnes lake	12	48.56	0.00	23.27	89	0.2	11.1	405.3	349.4	239.7	20.9	7.21	77	266.79	594.01
Hearnes lake	13	34.88	0.00	7.11	95	0.2	5.0	466.3	214.3	188.8	27.2	7.18	66	132.79	375.71
Hearnes lake	14	32.90	0.00	4.77	96	0.2	3.6	412.8	176.1	197.4	22.3	8.11	83	104.29	136.34

Hearnes lake	15	41.15	0.00	1.00	99	0.0	0.6	340.2	109.9	112.7	22.4	8.05	95	201.07	448.02
Pine brush creek	1	80.10	0.03	4.43	97	1.1	1.5	800.3	161.8	1441.7	24.0	7.11	74	12.18	149.83
Pine brush creek	2	82.53	0.03	5.74	97	1.4	1.8	785.1	177.0	1575.7	25.0	7.08	74	10.00	87.76
Pine brush creek	3	81.23	0.03	4.95	97	1.3	1.5	1114.7	185.8	1979.5	30.1	6.70	74	8.64	182.63
Pine brush creek	4	97.33	0.03	5.63	97	1.1	1.5	1082.7	180.1	1561.2	30.9	6.92	82	6.57	184.84
Pine brush creek	5	111.02	0.06	5.55	97	1.8	1.3	1014.8	172.6	2649.5	26.3	6.90	50	6.36	150.99
Pine brush creek	6	72.31	0.04	4.52	97	1.7	1.6	931.7	180.7	2288.6	26.1	6.77	61	7.43	132.96
Pine brush creek	7	86.48	0.03	4.04	98	1.3	1.2	800.3	155.1	1549.2	22.1	6.85	69	6.86	84.01
Pine brush creek	8	114.97	0.05	5.13	97	1.5	1.1	1063.4	172.2	2408.6	22.3	6.82	59	6.43	147.16
Pine brush creek	9	125.86	0.05	5.99	97	1.3	1.2	1164.2	182.3	2287.8	24.6	6.79	57	8.36	246.24
Pine brush creek	10	158.64	0.04	6.28	98	0.9	1.0	1397.9	185.3	1958.1	23.1	6.81	69	9.71	105.61
Pine brush creek	11	81.63	0.03	4.28	97	1.3	1.3	702.6	153.2	1353.6	22.0	6.94	66	12.29	170.72
Pine brush creek	12	48.97	0.01	4.29	97	0.5	2.2	399.0	144.8	361.5	20.5	7.27	91	38.79	197.41
Pine brush creek	13	43.10	0.01	2.68	97	0.9	1.6	486.5	141.2	711.8	20.9	7.13	92	13.86	129.51
Pine brush creek	14	25.51	0.00	2.36	97	0.5	2.4	338.8	136.3	293.0	23.7	8.33	97	15.79	151.82
Pine brush creek	15	35.22	0.00	2.67	98	0.4	1.9	309.8	127.1	231.5	20.9	8.09	85	17.07	150.57
Pine creek	1	111.91	0.05	0.89	98	1.3	0.2	1611.6	119.3	3748.5	22.3	6.50	23	0.57	254.67
Pine creek	2	154.64	0.06	1.23	98	1.4	0.2	2457.2	129.5	5091.8	24.6	6.23	5	0.93	357.93
Pine creek	3	129.79	0.07	0.45	98	1.9	0.1	2365.5	111.5	6434.8	26.8	6.09	21	0.29	237.70
Pine creek	4	117.16	0.03	0.17	99	0.8	0.0	1873.3	104.0	2241.9	24.5	6.47	15	0.07	219.35
Pine creek	5	106.01	0.06	0.91	98	2.0	0.2	1628.6	121.3	4982.9	23.3	6.26	21	0.43	262.14
Pine creek	6	77.46	0.01	0.75	99	0.3	0.3	1328.0	118.8	761.2	24.0	6.47	29	0.36	258.06
Pine creek	7	78.26	0.03	0.45	98	1.4	0.1	1164.6	110.4	2529.6	21.8	6.56	19	4.14	243.62
Pine creek	8	63.69	0.01	0.80	99	0.7	0.3	1011.9	118.6	1044.2	23.2	6.18	25	0.00	207.23

Pine creek	9	78.88	0.02	0.41	99	0.7	0.1	1271.0	109.8	1300.2	24.1	6.40	13	0.00	215.43
Pine creek	10	181.81	0.15	0.75	97	2.8	0.1	2334.3	115.5	10529.1	22.0	6.41	26	0.14	573.41
Pine creek	11	153.34	0.12	1.10	97	2.6	0.2	1974.7	122.9	8439.2	21.3	6.37	11	0.29	431.24
Pine creek	12	109.78	0.05	1.32	98	1.5	0.3	1225.6	123.7	2913.2	19.5	6.61	38	0.93	373.71
Pine creek	13	117.52	0.07	1.21	98	2.1	0.3	1612.1	127.3	5522.3	19.8	7.10	22	0.29	92.92
Pine creek	14	116.07	0.03	0.82	99	0.9	0.2	1522.9	117.8	2273.0	19.3	7.07	37	0.07	128.10
Pine creek	15	94.34	0.02	1.43	99	0.9	0.4	1070.0	125.4	1481.1	20.6	6.87	38	0.14	123.22
Woolgoolga lake	2	70.95	0.04	21.33	93	1.9	5.2	919.5	448.6	2580.7	25.3	7.03	55	48.90	301.39
Woolgoolga lake	3	75.65	0.01	1.17	99	0.6	0.4	1337.0	127.2	1189.1	28.1	6.80	73	1.29	256.90
Woolgoolga lake	4	43.69	0.01	0.49	99	0.8	0.3	748.3	109.7	764.0	30.0	7.06	51	0.21	339.82
Woolgoolga lake	5	42.34	0.01	0.79	98	1.2	0.5	675.7	115.9	1075.2	27.4	7.06	37	0.36	224.34
Woolgoolga lake	6	32.03	0.01	0.77	98	1.4	0.6	599.6	116.7	1108.4	28.7	7.05	54	0.14	295.20
Woolgoolga lake	7	52.17	0.11	0.71	93	6.7	0.3	776.7	114.1	7274.9	26.5	7.07	29	0.00	279.21
Woolgoolga lake	8	55.39	0.10	0.72	94	5.9	0.3	741.1	113.6	6307.5	24.0	7.02	24	0.21	306.14
Woolgoolga lake	9	49.65	0.04	0.61	97	2.5	0.3	707.2	111.6	2386.8	25.8	6.80	22	0.43	318.17
Woolgoolga lake	10	89.88	0.03	1.01	99	1.1	0.3	1036.1	116.3	1592.9	27.0	6.99	120	0.00	322.25
Woolgoolga lake	11	112.45	0.20	0.25	94	5.8	0.1	1386.5	104.5	11875.1	26.3	6.75	33	0.00	283.75
Woolgoolga lake	12	121.34	0.01	86.81	84	0.1	15.7	1095.1	1292.0	360.5	22.5	6.88	56	162.86	431.95
Woolgoolga lake	13	81.50	0.00	50.13	86	0.1	13.8	1077.2	1105.2	362.8	22.3	6.81	67	171.36	365.22
Woolgoolga lake	14	60.32	0.00	33.58	87	0.0	12.7	799.8	748.1	107.8	22.6	7.55	60	72.21	308.27
Woolgoolga lake	15	113.66	0.02	93.85	82	0.5	17.7	1099.6	1486.5	1044.8	22.2	7.72	73	227.43	396.69